# Effect of Type and Content of Expansive Agent on Performance of Fiber-Reinforced Concrete with Adapted Rheology

Ahmed Abdelrazik

Kamal Khayat
*Missouri University of Science and Technology*, khayatk@mst.edu

Construction and Building Materials 314 (2022) 125610

Contents lists available at ScienceDirect

Construction and Building Materials

journal homepage: www.elsevier.com/locate/conbuildmat

# Effect of type and content of expansive agent on performance of fiber-reinforced concrete with adapted rheology

Ahmed Abdelrazik [a,b], Kamal H. Khayat [a,*]

[a] *Missouri University of Science and Technology, United States*

[b] *Structural Engineering Department, Faculty of Engineering, Ain Shams University, Cairo, Egypt*

A R T I C L E I N F O

*Keywords:*
Expansive agent
Restrained shrinkage
Self-consolidating concrete
Shrinkage
Steel fibers
Synergetic effect

A B S T R A C T

A performance-based mixture design approach was utilized to optimize the binder content and composition for fiber-reinforced super workable concrete (FR-SWC) and fiber-reinforced self-consolidating concrete (FR-SCC). The test parameters included the replacement ratio of the cement by a Class C fly ash (FA), type and content of expansive agent (EA), and total binder content. Hooked-end steel fibers measuring 30 mm in length were used at 0.5% by volume. The investigated concrete was tested for slump flow, modified J-ring, sieve stability, bleeding, visual stability index, air content, unit weight, as well as compressive and splitting tensile strengths. The elastic modulus, autogenous, drying shrinkage, and restrained shrinkage were determined for optimized mixtures. The optimized binder content for the FR-SCC mixtures was 475 kg/m$^3$ with 30% FA replacement, by mass of total binder. For the FR-SWC mixtures, the binder content was 380 kg/m$^3$ binders with 30% FA, by mass. In both mixture types, a Type-G EA was incorporated at 4% by binder mass.

Test results indicated that a sharp loss in filling ability was obtained in mixtures made with a Type-K EA compared to those made with a Type-G or no EA. The coupled used of fibers and EA resulted in a slight increase in compressive strength for the FR-SCC but considerable improvement in compressive strength (up to a 50%) in the case of FR-SWC. The FR-SCC and FR-SWC mixtures exhibited up to 55% and 80% greater splitting tensile strength, respectively, compared to the non-fibrous concrete. The combination of steel fiber and EA significantly reduced shrinkage, up to 65% lower shrinkage after one year for the FR-SCC and FR-SWC mixtures. An increase in restrained shrinkage resistance was observed when the EA or fiber was used in proportioning the FR-SCC. Combined use of fibers and 4% Type-G EA led to the highest reduction in cracking potential that decreased from relatively high to low level with the time-to-cracking increasing from 12.5 to 36.5 days.

## 1. Introduction

Self-consolidating concrete (SCC) mixture design requires the use of high cement paste, which can lead to greater shrinkage and greater cracking risk compared to conventional vibrated concrete (CVC). Proper design of the SCC requires high filling capability, high passing capability, and high stability. This requires a relatively high paste content that may increase the risk of shrinkage and cracking. Super-workable concrete (SWC) is a new high-performance concrete (HPC) class with an adapted rheology that can be combined with a lower paste compared to SCC [1]. In contrast to SCC, SWC requires some consolidation to ensure a sufficient filling of the formwork, which is considerably lower than CVC [2]. Compared to SCC, SWC may exhibit a lower risk of cracking due to shrinkage. Below is a summary of the literature to help understanding the effect of fibers and expansive agent (EA), there combined effect, as well as the supplementary cementitious materials (SCMs) on the shrinkage and cracking resistance behavior of fiber-reinforced concrete (FRC).

The incorporation of EA, such as a Type-G EA based on CaO or MgO, can lead to some initial expansion that can compensate for drying shrinkage [3]. Peiwei et al. [3] evaluated the effect of CaO- and MgO-based EAs on the shrinkage of roller compacted concrete. The EA dosage varied between 4% and 12% of the mass of cement. The authors reported that it took 3 and 28 days for the CaO- and MgO-based EAs, respectively, to attain a maximum expansion. The incorporation of fibers in concrete is an effective method that can reduce or prevent concrete cracking. Fibers can reduce crack width ($W_{cr}$) once cracking takes place or increase the crack bearing capacity [2]. Sun et al. [4] evaluated

* Corresponding author.
*E-mail address:* khayatk@mst.edu (K.H. Khayat).

https://doi.org/10.1016/j.conbuildmat.2021.125610
Received 24 October 2020; Received in revised form 30 October 2021; Accepted 7 November 2021
Available online 16 November 2021

the effect of fibers combined with EA on the permeability and shrinkage of concrete. The authors proposed HPC made with EA and different types of hybrid fibers including steel, polyvinyl alcohol, and polypropylene fibers. The HPC made with EA and fibers produced the best results in reducing shrinkage and permeability compared to HPC made with hybrid fibers or EA alone. The mixture made with 12% EA and hybrid fibers had a relative penetration coefficient of $0.127 \times 10^{-7}$ cm/h compared to $0.59 \times 10^{-7}$ and $2.9 \times 10^{-7}$ cm/h for the fibrous mixture made without EA and the nonfibrous mixture made without EA, respectively. The mixture made with 12% EA and hybrid fibers and the fibrous mixture made without EA exhibited reduction in the 120-day shrinkage by up to 70% and 40%, respectively.

Kassimi and Khayat [5] studied the combined effect of fibers, EA as well as shrinkage-reducer admixture (SRA) on the cracking resistance of different fiber-reinforced self-consolidating concrete (FR-SCC) mixtures using the restrained shrinkage test. The investigated parameters included the incorporation of EA or SRA, fiber volume ($V_f$) (0 and 0.5%), and fiber type (polypropylene and steel fibers). The lowest cracking potential was observed with FR-SCC made with the steel fibers combined with EA that had to a net time-to-cracking ($t_{cr}$) of 36 days (low cracking potential according to [6]). Such concrete also exhibited the lowest $W_{cr}$ of 83 μm at the time of cracking compared to 160 μm for the SCC without EA or fiber that cracked after 2.6 days, which reflects high cracking potential [6]. The mixtures included in such study included four mixtures with four different water-to-cementitious materials ratios (w/cm). Two were normal-strength concrete with w/cm of 0.45 and 0.55. The other two were HPC mixtures prepared with w/cm of 0.35 and 0.30. Pan et al. [7] studied the effect of the combination of two types of EAs, CaO- based and ettringite-based EAs, on high performance FRC. The investigated fiber type included polyvinyl alcohol fiber, cellulose fiber, and polypropylene fiber. The slump for the investigated concrete was fixed at 200 mm. The results showed that the fibrous concrete prepared with the combined EAs at a content of 7% to 8%, by mass of binder, exhibited good workability and high durability and early cracking resistance with limited effect on slump and compressive strength. Cao et al. [8] investigated the effect of fibers and EA, separately and simultaneously, on plastic shrinkage of FR-SCC slabs. Fibers included steel fiber volume ($V_f$) used at 0.25%, 0.5% and 0.75%, polypropylene fibers employed at 0.05%, 0.1% and 0.15%, as well as hybrids fibers. An EA was introduced at 6% and 8% by mass of the binder. The expansive FR-SCC was shown to develop 70% higher crack reduction factor compared to the non-expansive FR-SCC. Li et al. [9] investigated the workability, shrinkage characteristics, and mechanical properties of FR-SCC prepared with or without calcium-sulfoaluminate EA (Type-K) employed at 10% by mass of binder. The steel fiber volume fraction varied from 0.4% to 1.2%. The authors reported that the expansion of the FR-SCC was inversely proportional to the volume of steel fibers. The compressive strength was enhanced slightly by only 5%. On the other hand, the splitting tensile strength was increased by up to 60%, and the drying shrinkage was reduced by up to 70% with the increase of fiber content. Cao et al. [10] performed shrinkage tests for FR-SCC mixtures prepared with different EA dosages (6%, 8%, 10%, and 12%) and different fiber types and volumes, which included steel fibers with $V_f$ of 0.25% to 0.75%, polypropylene fibers with $V_f$ of 0.05% to 0.15%, and hybrid fibers 0.25% steel with 0.1% polypropylene and 0.5% steel with 0.05% polypropylene. Shrinkage testing was performed under two different curing conditions, sealed curing and top-surface exposure curing. The results proved that the curing condition has a significant effect on shrinkage and expansion of FR-SCC, where the shrinkage under top-surface exposure cure was 5 to 10 times greater than that under sealed curing condition. Under any of the two curing conditions and for FR-SCC prepared with steel or polypropylene fibers, the expansion and shrinkage of FR-SCC was significantly less than SCC prepared without fibers. The steel fibers had higher effect on reducing the expansion of FR-SCC compared to polypropylene fibers. Meanwhile, the later had higher effect on reducing shrinkage. Corinaldesi et al. [11] studied the effectiveness of using Type-G EA at dosages varying between 0, 20, and 40 kg/m$^3$ on mechanical characteristics of different engineered cement-based composites (ECCs) prepared with 100 kg/m$^3$ of ribbon-shaped amorphous metallic steel fibers. The mechanical properties including compressive and flexural strengths were directly proportional to the EA dosage that was optimized at 40 kg/m$^3$. Polymetric fibers were added in combination with steel fibers and the optimized EA dosage. The polymetric fibers included hooked and corrugated polyethylene terephthalate, and polyvinyl alcohol, where each of these fibers were introduced combined with steel fibers at ratios 100/0, 75/25, 50/50, 25/75, and 0/100. The variation of fiber combination did not significantly affect the fluidity or compressive strength of the ECCs. On the other hand, the variation hybrid system strongly affected the flexural behavior where mixtures prepared with only steel fibers had significantly higher first crack stress compared to non-fibrous concrete. The first crack stress was directly proportional to the ratio of steel fibers. One the other hand, mixtures having higher ratios of steel fibers had lower residual stress to first crack stress ratio. The mixtures prepared with only polypropylene fibers had residual stress even higher than the first crack stress. Park et al. [12] investigated the effect of combined calcium sulphoaluminate EA and glycol-based SRA on the compressive and tensile strength as well as shrinkage of ultra-high-performance concrete (UHPC). Concrete was prepared using 13-mm long straight steel fibers used at 15.6 kg/m$^3$ ($V_f = 2\%$). The authors reported that the combined use of EA and SRA had negligible effect on compressive strength, about 10% increase in tensile strength, and significant drop in shrinkage of about 80% after 1 day and 75% after 21 days.

The presence of SCMs in concrete mixture can influence the expansion characteristics of SCC and SWC made with EA. The effect of EA in reducing shrinkage is enhanced by increasing the SCMs content [13]. Peiwei et al. [14] investigated the effect of fly ash (FA) and MgO based EA on the shrinkage and expansion behavior of concrete made with high magnesia cement. The results showed that the use of FA decreased shrinkage and expansion produced by the MgO-Type EA. The shrinkage strain of concrete with 50% FA replacement was about 33% less than that of specimens made without any FA. Zhang and Li [15] studied the effect of slag cement and FA on restrained expansion and compressive strength of concrete made with sulphoaluminate-based EA. Both restrained expansion rate and strength decreased with the use of SCM and EA. Aiguo et al. [16] studied the effect of the combination of steel fibers and MgO-Type EA on expansion, compressive strength, splitting tensile strength, permeability, and porosity of concrete. Expansion caused by the use of MgO-Type EA under restrain of fibers decreased the pore volume and pore size. The pore volume determined in the mortar fraction of the steel fiber-reinforced concrete (FRC) made with MgO-Type EA decreased by 39% compared to that containing EA only. Compressive and splitting tensile strengths of concrete made with fibers and EA were found to increase by approximately 20% and 55%, respectively, at 7 days and 15% and 40%, respectively, at 28 days, compared to non-FRC concrete. The 28-day permeability coefficient, $K_t$, depth of penetration, $L$, and porosity of concrete decreased by about 40%, 20%, and 15%, respectively.

The incorporation of fibers into SCC can limit workability, especially beyond a certain $V_f$ (e.g., 0.5%) [2]. SWC is placed with some mechanical consolidation and is prepared with a lower binder content than SCC and can be proportioned with $V_f$ up to 0.75% without significant drop of workability [2]. Another benefit of using fiber-reinforced super workable concrete (FR-SWC) over FR-SCC, is the lower risk of shrinkage due to the higher aggregate-to-binder ratio of the FR-SWC.

Abdelrazik and Khayat [17] studied the workability of FR-SCC and FR-SWC prepared with various fiber types (steel fibers, polypropylene fibers, and hybrid fibers) and volumes, with $V_f$ varying between 0 and 0.75%. The workability assessment included passing ability using modified J-Ring test and stability using VSI, surface settlement test, and bleeding assessment. Results indicated that FR-SCC and FR-SWC prepared with 0.5% steel fibers can exhibit the optimum workability in

terms of concrete high fluidity, passing ability and stability. These findings are in agreement with Kassimi [2].

For proper filling capacity of the formwork, limited degree of mechanical consolidation of the SWC is required. Khayat et al. [18] studied the effect of the degree of mechanical consolidation of FR-SWC on stability and strength. The study included the casting of 100 × 200 mm cylindrical specimens. The specimens were cast in a single layer and consolidated using a 10 mm rod for a different number of strokes, as well as mechanical consolidation using a vibrating table for 20 and 25 s. Image analysis was conducted on longitudinal saw-cut surfaces to assess segregation as a function of consolidation mode. The surface quality of the samples was also investigated for signs of bleeding and honeycombing, and the samples were tested for compressive strength. The authors found that casting cylinders in one layer and consolidating them with 20 strikes can lead to adequate performance.

Highly flowable yet stable FR-SCC has been used as a repair material in some repair projects [19]. Similarly, FR-SWC was used a construction material for locations where high tensile stresses are anticipated, and relatively high concentration of steel reinforcement is located, thus necessitating the use of highly flowable concrete [20]. Achieving optimum mixture proportioning for FR-SCC and FR-SWC with shrinkage compensating characteristics necessitates good understanding of the coupled effect of type and dosage of EA and fibers on workability, mechanical properties, and shrinkage. This paper summarizes an experimental program to optimize mixture proportioning of FR-SCC and FR-SWC prepared with different types/contents of EA combined with Class C FA at different contents based on fresh and mechanical properties, as well as the shrinkage behavior, including restrained shrinkage.

## 2. Experimental program

### 2.1. Materials

A Type I/II ordinary portland cement (OPC) and a Class C FA were used. Two types of EA were used: a CaO-based system (Type-G EA) and a calcium sulfoaluminate-based system (Type-K EA). The Type-G EA reacts with water forming calcium hydroxide ($Ca(OH)_2$) crystals that causes the expansion, while expansion by the Type-K EA is due to formation of ettringite. The Type-G EA can be affected by the burning temperature and other parameters of the CaO (e.g. partial size distribution). In this study, commercially available CaO-based EA (CONEX® ) was selected within the recommended range of content of this material. CONEX® is a powdered additive that is used to compensate for and reduce net shrinkage in Portland Cement concrete. The development of an expanding component is its functional mechanism. CONEX® is a Type G component that forms a calcium hydroxide platelet crystal structure in accordance with ACI 223 specifications. Table 1 summarizes mineral and chemical compositions of cement, fly ash and expansive agents used in this study. The CaO existing in Portland cement and Class C FA is free lime that survives processing without reacting in building products, while the CaO existing in Type-G EA is quicklime that reacts directly with water to produce $Ca(OH)_2$.

**Table 1**
Chemical compositions of cement, fly ash and expansive agents.

| | OPC | Class C FA | K-Type EA | G-Type EA |
|---|---|---|---|---|
| $SiO_2$ % | 19.8 | 36.5 | 7.7 | 11.8 |
| $Al_2O_3$ % | 4.5 | 24.8 | 7 | 3.7 |
| $Fe_2O_3$ % | 3.2 | 5.2 | 1.2 | 0.9 |
| CaO % | 63.1 | 26 | 50.1 | 82.6 |
| MgO % | 2.7 | 5 | 0.1 | 0.1 |
| $SO_3$ % | 3.4 | 2.5 | 33.3 | – |
| $Na_2O$ eq. % | – | – | 0.6 | 0.9 |
| $CaCO_3$ % | 3.3 | – | – | – |
| Blaine surface area, $m^2/kg$ | 390 | 498 | – | – |
| Denisty | 3.14 | 2.71 | 2.9 | 3.1 |
| LOI % | 1.5 | 0.5 | 2.1 | – |

As a fine aggregate for both FR-SCC and FR-SWC, natural sand with continuous grading, fineness modulus of 2.6, specific gravity of 2.63, and water absorption of 0.62% was used. For the FR-SWC, Coarse aggregate used was crushed limestone that had a nominal maximum size of 12.5 mm, specific gravity of 2.8, and water absorption of 3.08%. For the FR-SWC, pea gravel that had a nominal maximum size of 10 mm, specific gravity of 2.54, and water absorption of 3.81% was used as the coarse aggregate. A high slump retention polycarboxylate-based high-range water reducer (HRWRA) was used. The HRWRA dosage was adjusted to secure slump flow between 650 and 700 mm for the FR-SCC and 500 to 550 mm for the FR-SWC. A synthetic resin-based air-entraining admixture (AEA) was incorporated to secure an initial air content of 6% to 9%. A polysaccharide viscosity-modifying admixture (VMA) was used for stability enhancement. A 30-mm long steel fiber with hooked ends and an equivalent diameter of 0.55 mm (aspect ratio 0.55) was used.

### 2.2. Test methods

All of the investigated mixtures were tested for slump flow and VSI (ASTM C 1611) [21].

Optimized mixtures were further tested for air content after 10 and 70 min. The concrete was agitated at 1 rpm in the mixer between the test periods. Using the modified J-Ring test [22], the initial passing ability was determined. Unlike the standard ring test (ASTM C 1621) [23], the modified J-Ring consists of a ring with eight bars not 16 bars. Bleeding (ASTM C 232) [24], sieve stability [25], air content (ASTM C 138) [26], and unit weight (ASTM C 231) [27] were also determined.

Using 100 × 200 mm cylinders, elastic modulus, splitting tensile strength, and compressive strength were evaluated after 28 and 56 days of moist curing that were tested according to ASTM C 39 [28], C 496 [29], and C 469 [30], respectively. The FR-SWC samples were cast in one lift and rodded 20 times using 10-mm steel rods [22].

Three 75 × 75 × 285 mm prismatic specimens were taken from each mixture for drying shrinkage measurements in accordance with ASTM C 157 [31]. The prisms were cured for 7 days then stored at relative humidity of 50% ± 4% and temperature of 23 ± 1.7 °C. Autogenous shrinkage was also measured in accordance with ASTM C1698 [32]. Mortar sieved from the fibrous concrete was used to fill corrugated deformable plastic tubes to measure autogenous shrinkage. A digital type extensometer was employed for both autogenous and total shrinkage measurements. The prisms were stored at 23 ± 1.7 °C. Autogenous and total shrinkage were monitored for one year. The total shrinkage reported in this study is calculated as the sum of the autogenous shrinkage determined after one day of age, that corresponds to the time of demolding of the drying shrinkage specimens, and the drying shrinkage/expansion recorded after the first day of age.

Restrained shrinkage was evaluated in accordance with ASTM C1581 [33]. As shown in Fig. 1, The test consisted of two 150-mm high concentric rings: an inner steel ring with a thickness of 12.5 mm and a diameter of 330 mm, and an outer cardboard ring measuring 406 mm in diameter and thickness 2 mm. Concrete was cast between the two rings with thickness 36 mm. The bolts with eccentric washers were immediately loosened as soon as the test specimens were transferred to the testing room (humidity and temperature -controlled room with a relative humidity of 50% ± 4% and temperature of 23 ± 1.7 °C). The washers were then rotated so they are not in contact with neither the cardboard nor steel rings. The concrete samples were left to cure for 3 days by covering them with wet burlap. Stress development induced by the restrained shrinkage of the concrete was monitored by three strain gauges attached to the inner surface of the steel. The steel strain was recorded directly after casting the rings using a data accusation system that records readings every 20 min until the concrete cracked. A sudden decrease in strain indicated cracking of the concrete sample. The first crack width was measured for all the rings using an optical crack meter

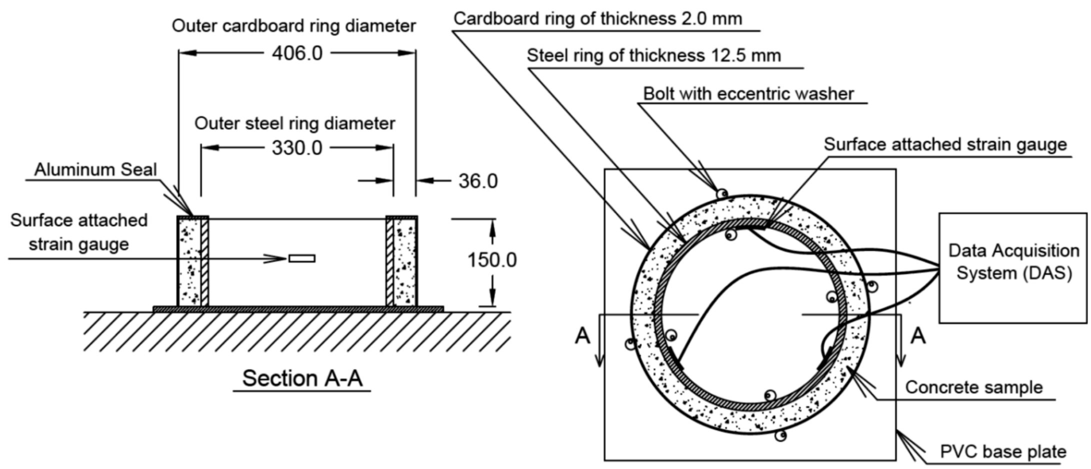


**Fig. 1.** Test setup for restrained shrinkage test (Ring test).

since the first crack was inspected. The crack width was measured on daily basis up to the end of the test (50 days).

## 3. Mixture proportioning

The mixture proportioning is based on the approach proposed by Voigt et al. [34] to calculate the average thickness of the matrix layer ($t_m$) enveloping fibers and coarse aggregate particles based on the multi-aspect concept as represented by Equation (1). The average thickness of the matrix covering the fibers and the aggregate was expressed using Equation (2). This involved an increase in mortar content to maintain the same thickness of mortar around the coarse aggregates and fibers in the FRC compared to the non-fibrous mixture.

$$t_m = \frac{Volume\ of\ Excess\ Matrix}{Total\ Surface\ Area\ of\ Fibers\ and\ aggregates} \quad (1)$$

$$t_m = \frac{V_c - V_g - V_f - V_v}{A_g + A_f} \quad (2)$$

where $t_m$ = average thickness of matrix covering coarse aggregate and fibers, $V_f$ = volume of fibers, $V_g$ = volume of coarse aggregate, $V_c$ = volume of concrete, $V_v$ = volume of voids in the coarse aggregate and fiber skeleton, $A_f$ = total surface area of fibers, and $A_g$ = total surface area of coarse aggregate. The volume of voids was obtained by determining the packing density of the mixture of coarse aggregate and fibers according to ASTM C 29 [35]. This approach was conducted to adjust the mixture proportioning of the FR-SCC and the FR-SWC based on the SCC and SWC mixture design, respectively.

The total surface area of fibers was calculated based on geometry of the fiber and fiber volume (0.5%). The grain-size distribution of coarse aggregate was divided into number (n) of group sizes then Equation (3) and (4) were used to compute the total (specific) surface area of coarse aggregate.

$$A_g = K.Vol_g \quad (3)$$

$$whereK = 6\left\{\frac{\%_{g1}}{d_1} + \frac{\%_{g2}}{d_2} + \frac{\%_{g3}}{d_3} + \frac{\%_{g4}}{d_4} + \cdots + \frac{\%_{gn}}{d_n}\right\} \quad (4)$$

where $d_1$ = diameter of coarse aggregate in group size 1; $\%_{g1}$ = ratio of coarse aggregate with $d_1$, etc.

The total surface area of fibers ($A_f$) can be calculated using Equation (5) [2]:

$$A_f = \frac{4 \times V_f}{d_f} \quad (5)$$

where $V_f$ is the fiber volume in a cubic meter of concrete.

The mixture proportioning of the FR-SCC and FR-SWC was determined using the following five steps:

(1) The factor $K$ was calculated using Equation (4).
(2) The specific surface area of coarse aggregates was calculated using Equation (2).
(3) The specific surface area of fibers was calculated using Equation (5).
(4) The mortar thickness of the non-fibrous mixtures was estimated using Equation (6).

$$t_{mortarbefore} = \frac{Vol_c - Vol_{gb} - Vol_{vb}}{A_{gb}} = t \quad (6)$$

where $Vol_c$ = volume of concrete (1 m$^3$); $Vol_{gb}$ = volume of coarse aggregate before adding fibers; $A_{gb}$ = total surface area of coarse aggregate before adding fibers; $Vol_{vb}$ = volume of voids in the coarse aggregate skeleton before adding fibers.

(5) The sand and coarse aggregate volumes after adding fibers were calculated using Equations (7) and (8).

$$V_g = \frac{Vol_c - Vol_v - tA_f}{tK + 1} \quad (7)$$

$$Vol_{sb} + Vol_{gb} = Vol_s + Vol_g + Vol_f \quad (8)$$

where $Vol_{sb}$ = volume of sand before adding fibers; $Vol_v$ = volume of voids in the coarse aggregate and fibers skeleton.

### 3.1. Trial mixtures to optimize binder content and FA substitution rate

Table 2 shows the trial batches conducted to optimize the binder content for the FR-SWC mixtures made with 0.5% fiber and different contents of FA and EA. The VSI was monitored before sampling. Only mixtures with high stability and the lowest possible binder content (in the case of FR-SWC mixtures) were sampled for further evaluation of workability and mechanical properties. The FR-SWC mixtures were optimized with total binder content of 380 kg/m$^3$, except for the mixtures with EA and no FA that contained 420 kg/m$^3$ of binder. Four mixtures were retained for further analysis and had relatively low binder content and adequate stability, denoted by a VSI of 0 or 1.

### 3.2. Mixture proportioning and testing of optimized mixtures

The mixture parameters considered in this study included the replacement level of the cement by FA (0, 30%, and 50%), $V_f$ (0 and

**Table 2**
Mixture proportions of FR-SWC mixtures to select binder content and FA replacement

| Mixture | Fiber (%) | Binder (kg/m$^3$) | FA (%) | EA (%) | EA type | VSI |
|---|---|---|---|---|---|---|
| FR-SWC1a | 0.5 | 420 | 0 | 0 | – | 0 |
| FR-SWC1b | 0.5 | 400 | 0 | 0 | – | 0 |
| FR-SWC1c | 0.5 | 380 | 0 | 0 | – | 0 |
| FR-SWC1d* | 0.5 | 360 | 0 | 0 | – | 1 |
| FR-SWC2a | 0.5 | 380 | 30 | 0 | – | 0 |
| FR-SWC2b* | 0.5 | 360 | 30 | 0 | – | 1 |
| FR-SWC3a | 0.5 | 380 | 50 | 0 | – | 0 |
| FR-SWC3b* | 0.5 | 360 | 50 | 0 | – | 1 |
| FR-SWC4a | 0.5 | 380 | 0 | 8 | G | 2 |
| FR-SWC4b* | 0.5 | 420 | 0 | 8 | G | 0 |
| FR-SWC5a | 0.5 | 380 | 0 | 8 | K | 2 |
| FR-SWC5b* | 0.5 | 420 | 0 | 8 | K | 0 |
| FR-SWC6a | 0.5 | 400 | 30 | 8 | G | 0 |
| FR-SWC6b | 0.5 | 380 | 30 | 8 | G | 0 |
| FR-SWC7a | 0.5 | 400 | 30 | 8 | K | 0 |
| FR-SWC7b | 0.5 | 380 | 30 | 8 | K | 0 |

* Refer to mixtures retained for full investigation

0.5%), type of EA (G and K), and dosage of EA (0, 4%, and 8%), as shown in Table 3. Fiber volume of 0.5% was selected based on recommendations from Abdelrazik and Khayat [17] and Kassimi [2]. The w/cm of the 28 investigated mixtures was set at 0.42 ± 0.01 for all mixtures. The mixture proportioning of the selected reference SCC (SCC-0FA-0EA in Table 3) is based on recommendations offered by the author [18].

## 4. Experimental results and discussion

### *4.1. Fresh properties of optimized mixtures*

Table 4 summarizes the fresh properties and mechanical properties of the 28 investigated mixtures. The mixtures with 30% FA showed better workability compared to those without FA or with 50% FA. The fresh air volume varied between 6.1% and 9.0%. The loss of air content between 10 and 70 min did not exceed 0.5%. All mixtures were stable with a VSI of 0 or 1. Minor bleeding was observed for some mixtures, and was less than 1.15%. The sieve stability for all mixtures ranged from 2.2% to 8.5%, which can be considered as high stability [25]. The bleeding for the investigated mixtures ranged from 0 to 1.14%, which can be considered low bleeding.

The initial slump flow for the SCC and FR-SCC mixtures ranged from 660 to 700 mm and from 495 to 560 mm in the case of the SWC and FR-SWC mixtures. The use of a Type-K EA led to a high degree of workability loss compared to the mixtures made with Type-G EA or those made without any EA. The FR-SCC mixture without any EA had 22% drop in slump flow after 60 min. The FR-SCC mixture with 4% Type-G EA had 8% slump flow drop after 60 min compared to 50% in the case of FR-SCC made with 8% Type-K EA. This may be due to the rapid formation of ettringite that can lead to sharp loss in free water and workability. The Type-K EA contains cement mixed with anhydrous-Hauyne (3CaO·3Al2O3·CaSO4), quick lime (CaO), and gypsum (CaSO4). The chemical reaction of Type-K EA when mixed with water is shown in Equation (9), as reported by Nagataki and Gomi [36].

$$C_4A_3S + 8CaSO_4 + 6CaO + 96H_2O \text{ ——greater than } 3C_3A \cdot 3CaSO_4 \cdot 32H_2O \quad (9)$$

The ettringite formation ($3C_3A \cdot 3CaSO_4 \cdot 32H_2O$) consumes a lot of water ($96H_2O$) which can lead to the fast redaction in fluidity, thus reducing rapidly the workability of the concrete. This has been documented in the literature (Jakob et al. 2019), the loss of workability of the reacting cement paste was shown to be highly correlated with increasing ettringite content. The Krieger-Dougherty equation, which defines the influence of solid fraction on the viscosity of a suspension, was used to explain an exponential link between ettringite development and flow behavior [37].

Unlike Type-K EA, Type-G EA reactivity includes the formation of Ca(OH)$_2$ due to the reaction of (CaO) quicklime with water. Equation (10)

**Table 3**
Mixture proportions

| | Mixture abbreviation | Fiber (%) | Binder (kg/m$^3$) | FA (%) | EA (%) | EA type | Sand (kg/m$^3$) | Agg. (kg/m$^3$) | VMA (ml/m$^3$) | HRWR (ml/m$^3$) | AEA (ml/m$^3$) |
|---|---|---|---|---|---|---|---|---|---|---|---|
| SCC & FR-SCC | SCC-0FA-0EA | 0 | 475 | 0 | 0 | – | 745 | 747 | 4285 | 1430 | 140 |
| | SCC-30FA-0EA | 0 | 475 | 30 | 0 | – | 745 | 747 | 4285 | 1350 | 140 |
| | SCC-30FA-4G | 0 | 475 | 30 | 4 | – | 745 | 747 | 4285 | 1280 | 140 |
| | FR-SCC-0FA-0EA | 0.5 | 475 | 0 | 0 | – | 780 | 690 | 4285 | 1945 | 140 |
| | FR-SCC-30FA-0EA | 0.5 | 475 | 30 | 0 | – | 780 | 690 | 4285 | 1430 | 140 |
| | FR-SCC-50FA-0EA | 0.5 | 475 | 50 | 0 | – | 780 | 690 | 4285 | 1430 | 140 |
| | FR-SCC-0FA-4G | 0.5 | 475 | 0 | 4 | G | 780 | 690 | 4285 | 1760 | 140 |
| | FR-SCC-0FA-8G | 0.5 | 475 | 0 | 8 | G | 780 | 690 | 4285 | 1660 | 140 |
| | FR-SCC-0FA-4K | 0.5 | 475 | 0 | 4 | K | 780 | 690 | 4285 | 1890 | 140 |
| | FR-SCC-0FA-8K | 0.5 | 475 | 0 | 8 | K | 780 | 690 | 4285 | 1790 | 140 |
| | FR-SCC-30FA-4G | 0.5 | 475 | 30 | 4 | G | 780 | 690 | 4285 | 1335 | 140 |
| | FR-SCC-30FA-8G | 0.5 | 475 | 30 | 8 | G | 780 | 690 | 4285 | 1570 | 140 |
| | FR-SCC-30FA-4K | 0.5 | 475 | 30 | 4 | K | 780 | 690 | 4285 | 1660 | 140 |
| | FR-SCC-30FA-8K | 0.5 | 475 | 30 | 8 | K | 780 | 690 | 4285 | 1715 | 140 |
| SWC & FR-SWC | SWC-0FA-0EA | 0 | 380 | 0 | 0 | – | 860 | 850 | 2145 | 1070 | 140 |
| | SWC-30FA-0EA | 0 | 380 | 30 | 0 | – | 860 | 850 | 2100 | 850 | 140 |
| | SWC-30FA-4G | 0 | 380 | 30 | 4 | G | 860 | 850 | 2100 | 1045 | 140 |
| | FR-SWC-0FA-0EA | 0.5 | 380 | 0 | 0 | – | 905 | 765 | 2145 | 930 | 110 |
| | FR-SWC-30FA-0EA | 0.5 | 380 | 30 | 0 | – | 905 | 765 | 2145 | 1200 | 70 |
| | FR-SWC-50FA-0EA | 0.5 | 380 | 50 | 0 | – | 905 | 765 | 2145 | 1230 | 95 |
| | FR-SWC-0FA-4G | 0.5 | 420 | 0 | 4 | G | 880 | 715 | 2145 | 1930 | 100 |
| | FR-SWC-0FA-8G | 0.5 | 420 | 0 | 8 | G | 880 | 715 | 3570 | 1715 | 100 |
| | FR-SWC-0FA-4K | 0.5 | 420 | 0 | 4 | K | 880 | 715 | 2500 | 1645 | 65 |
| | FR-SWC-0FA-8K | 0.5 | 420 | 0 | 8 | K | 880 | 715 | 2500 | 1570 | 70 |
| | FR-SWC-30FA-4G | 0.5 | 380 | 110 | 4 | G | 905 | 765 | 2500 | 1270 | 70 |
| | FR-SWC-30FA-8G | 0.5 | 380 | 105 | 8 | G | 905 | 765 | 2500 | 1185 | 85 |
| | FR-SWC-30FA-4K | 0.5 | 380 | 110 | 4 | K | 905 | 765 | 2500 | 1230 | 80 |
| | FR-SWC-30FA-8K | 0.5 | 380 | 105 | 8 | K | 905 | 765 | 2500 | 1270 | 80 |

**Table 4**
Fresh and mechanical properties

| | Mixture Code | VSI | flow 10 min. (mm) | flow 70 min. (mm) | Unit weight (kg/m$^3$) | Air 10 min. (%) | Air 70 min. (%) | D/a 10 min. | Bleeding (%) | Sieve Stab. (%) | $f_c$' 28 d (MPa) | $f_c$' 56 d (MPa) | $f_t$ 28 d (MPa) | $f_t$ 56 d (MPa) |
|---|---|---|---|---|---|---|---|---|---|---|---|---|---|---|
| | SCC-0FA-0EA | 0 | 680 | 510 | 2198 | 6.6 | 6.5 | 21.8 | 0.43 | 6.5 | 32.5 | 37.1 | 2.1 | 2.9 |
| SCC & FR-SCC | SCC-30FA-0EA | 0 | 670 | 530 | 2155 | 8.0 | 8.1 | 22.0 | 0.33 | 6.8 | 33.1 | 39.1 | 2.0 | 3.1 |
| | SCC-30FA-4G | 0 | 675 | 580 | 2145 | 8.2 | 8.1 | 22.3 | 0.1 | 6.1 | 36.9 | 39.9 | 2.2 | 3.2 |
| | FR-SCC-0FA-0EA | 0 | 660 | 530 | 2158 | 7.6 | 7.8 | 12.7 | 0 | 3.9 | 26.9 | 39.2 | 3.6 | 3.7 |
| | FR-SCC-30FA-0EA | 0 | 670 | 520 | 2218 | 6.6 | 6.9 | 13.1 | 0.74 | 4.4 | 36.8 | 39.2 | 4.2 | 4.4 |
| | FR-SCC-50FA-0EA | 0 | 670 | 510 | 2185 | 5.7 | 5.1 | 13.5 | 1.14 | 6.0 | 19.0 | 24.3 | 3.1 | 3.1 |
| | FR-SCC-0FA-4G | 0 | 665 | 600 | 2210 | 6.8 | 6.4 | 12.7 | 0.68 | 2.3 | 25.7 | 37.6 | 4.6 | 4.3 |
| | FR-SCC-0FA-8G | 0 | 665 | 560 | 2189 | 7.5 | 7.9 | 12.6 | 0.07 | 6.0 | 28.5 | 32.9 | 3.0 | 3.1 |
| | FR-SCC-0FA-4 K | 0 | 670 | 410 | 2166 | 6.5 | 6.9 | 12.3 | 0 | 3.2 | 29.4 | 33.0 | 2.9 | 3.2 |
| | FR-SCC-0FA-8 K | 0 | 670 | 330 | 2243 | 6.2 | 6.3 | 12.2 | 0.26 | 2.2 | 40.0 | 41.4 | 3.8 | 4.2 |
| | FR-SCC-30FA-4G | 0 | 690 | 640 | 2216 | 6.5 | 5.9 | 13.5 | 0.65 | 3.4 | 36.8 | 39.7 | 4.3 | 4.5 |
| | FR-SCC-30FA-8G | 0 | 680 | 610 | 2195 | 7.0 | 7.1 | 13.2 | 0.30 | 8.5 | 34.9 | 36.4 | 3.8 | 4.1 |
| | FR-SCC-30FA-4 K | 0 | 660 | 440 | 2221 | 6.2 | 6.3 | 12.7 | 0.18 | 8.5 | 37.5 | 39.7 | 3.2 | 3.3 |
| | FR-SCC-30FA-8 K | 0 | 700 | 350 | 2229 | 6.2 | 6.5 | 12.3 | 0.2 | 7.1 | 41.9 | 43.0 | 4.7 | 4.8 |
| SWC & FR-SWC | SWC-0FA-0EA | 0 | 510 | 280 | 2195 | 8.0 | 7.7 | 19.1 | 0 | 3.1 | 23.1 | 24.6 | 2.2 | 2.3 |
| | SWC-30FA-0EA | 0 | 500 | 275 | 2188 | 9.0 | 8.9 | 20.0 | 0 | 4.4 | 22.6 | 25.2 | 2.3 | 2.4 |
| | SWC-30FA-4G | 0 | 540 | 325 | 2175 | 8.7 | 8.8 | 20.0 | 0 | 3.7 | 27.5 | 31.7 | 2.6 | 3.3 |
| | FR-SWC-0FA-0EA | 0 | 500 | 290 | 2206 | 6.2 | 6.0 | 13.3 | 0 | 8.2 | 37.0 | 39.9 | 3.7 | 3.7 |
| | FR-SWC-30FA-0EA | 0 | 500 | 290 | 2234 | 5.8 | 5.8 | 14.5 | 0.34 | 6.3 | 35.0 | 39.7 | 3.5 | 3.9 |
| | FR-SWC-50FA-0EA | 0 | 540 | 280 | 2250 | 7.2 | 7.2 | 14.6 | 0.26 | 5.3 | 14.8 | 16.3 | 1.8 | 1.6 |
| | FR-SWC-0FA-4G | 0 | 530 | 210 | 2271 | 6.2 | 6.5 | 12.6 | 0.1 | 5.5 | 37.7 | 40.3 | 3.4 | 3.7 |
| | FR-SWC-0FA-8G | 1 | 560 | 190 | 2233 | 7.9 | 7.8 | 12.8 | 0.62 | 5.9 | 32.5 | 37.2 | 3.4 | 3.5 |
| | FR-SWC-0FA-4 K | 1 | 550 | 190 | 2210 | 6.8 | 6.3 | 12.4 | 1.1 | 3.8 | 36.1 | 39.9 | 3.6 | 4.0 |
| | FR-SWC-0FA-8 K | 0 | 495 | 180 | 2310 | 6.3 | 6.1 | 12.1 | 0 | 3.7 | 38.6 | 40.9 | 3.8 | 4.1 |
| | FR-SWC-30FA-4G | 0 | 550 | 260 | 2245 | 5.8 | 5.4 | 14.7 | 0.5 | 5.4 | 39.4 | 40.9 | 3.9 | 4.3 |
| | FR-SWC-30FA-8G | 0 | 550 | 240 | 2291 | 7.4 | 7.1 | 14.1 | 0.8 | 4.4 | 36.9 | 38.8 | 3.2 | 3.9 |
| | FR-SWC-30FA-4 K | 1 | 560 | 220 | 2245 | 6.5 | 6.6 | 13.8 | 1.0 | 4.0 | 39.2 | 40.3 | 3.7 | 4.1 |
| | FR-SWC-30FA-8 K | 0 | 510 | 210 | 2210 | 6.1 | 6.2 | 13.2 | 0 | 7.1 | 40.8 | 42.3 | 4.0 | 4.2 |

[36] shows such reactivity.

$$CaO + H_2O \rightarrow Ca(OH)_2 \quad (10)$$

As expected, the incorporation of fibers had a negative effect on passing ability; however, all of the FR-SCC and FR-SWC mixtures had acceptable passing ability index ($D/a$) greater than 12 [22]. Different binders' compositions did not have a considerable effect on the passing ability of either FR-SCC or FR-SWC mixtures ($12.1 < D/a < 14.7$).

## 4.2. Mechanical properties

Table 4 also summarizes the compressive and the splitting tensile strengths at 28 and 56 days for the 28 investigated mixtures. The 28-day compressive for the SCC and FR-SCC mixtures ranged from 19 to 41.9 MPa and from 14.8 to 40.8 MPa in the case of the SWC and FR-SWC mixtures. The 28-day splitting tensile strength for the non-fibrous SCC and SWC mixtures ranged from 2.0 to 2.2 MPa and from 2.2 to 2.6, respectively. The use of fibers had significant effect on the 28-day splitting tensile strength, where the FR-SCC and FR-SWC mixtures had splitting tensile strength up to 4.7 and 4.0 MPa, respectively. The 56-day compressive and splitting tensile strengths for the mixtures with 30% FA replacement were 60% and 40% higher than those with 50% FA replacement in FR-SCC, respectively. In the case of FR-SWC, the 56-day compressive and splitting tensile strengths for the 30% FA mixtures were 140% and 145% higher than those of 50% FA replacement, respectively. The FR-SCC mixtures made with EA and 30% FA replacement showed up to 20% and 30% increase in compressive and splitting tensile strengths, respectively, compared to mixtures with 0% FA replacement. Such increase was up to 5% and 15%, respectively, in the case of FR-SWC.

Similar to the findings from previous studies [16], Generally, the use

of EA had a positive effect on both compressive and splitting tensile strength. Mixtures made with 4% Type-G EA developed the highest splitting tensile strength in the case of FR-SWC (10% increase compared to FR-SWC made without any EA), while the 8% Type-K showed higher splitting tensile strength with FR-SCC (7% increase compared to FR-SCC made without any EA). Mixtures incorporating 8% Type-K EA showed the highest compressive strength for both concrete types; however, the difference in mechanical properties for the mixtures with 4% Type-G and Type-K was not significant. The use of fibers increased the splitting tensile strength by up to 40% and 60% in the case of FR-SCC and FR-SWC, respectively. The FR-SCC-50FA-0EA and FR-SWC-50FA-0EA mixtures were prepared with 50% FA and no EA and developed low 28-day compressive strength of 19.0 and 14.8 MPa. These mixtures were not selected for further analysis given the limited strength development. Mixtures with 30% FA replacements were selected for further testing of concrete with the two types of EA (Type-G and Type-K) incorporated at dosage ratios of 0%, 4%, and 8%, by mass of binder. The enhancement in the FRC strength due to the synergetic effect of

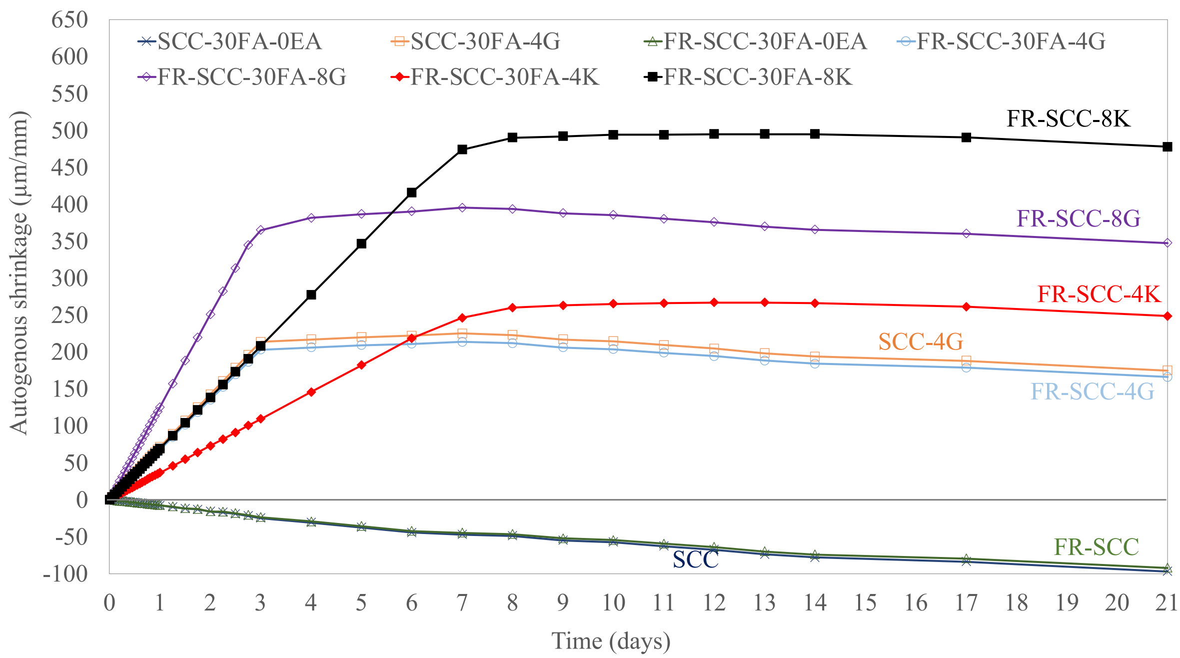


Autogenous shrinkage and expansion for selected FR-SCC mixtures up to 21 days (2-a)

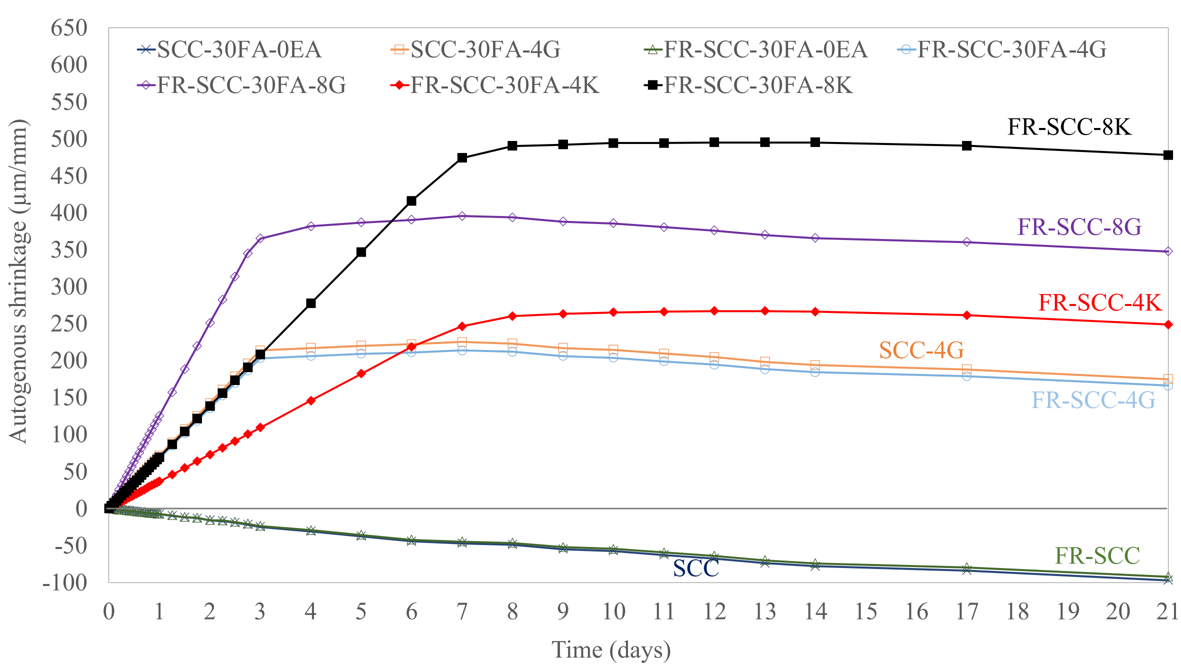


Autogenous shrinkage and expansion for selected FR-SCC mixtures up to 365 days (2-b)

**Fig. 2.** Autogenous shrinkage and expansion for selected FR-SCC mixtures. Autogenous shrinkage and expansion for selected FR-SCC mixtures up to 21 days (2-a), Autogenous shrinkage and expansion for selected FR-SCC mixtures up to 365 days (2-b).

fibers and EA can be explained by the expansion caused by the use of EA under restraining of fibers, which decreases the pore volume and pore size of the hydrated cement paste [16].

### *4.3. Shrinkage and expansion*

As mentioned in the previous section, the mixtures made with 30% FA replacement were selected over those mixtures made with 0% and

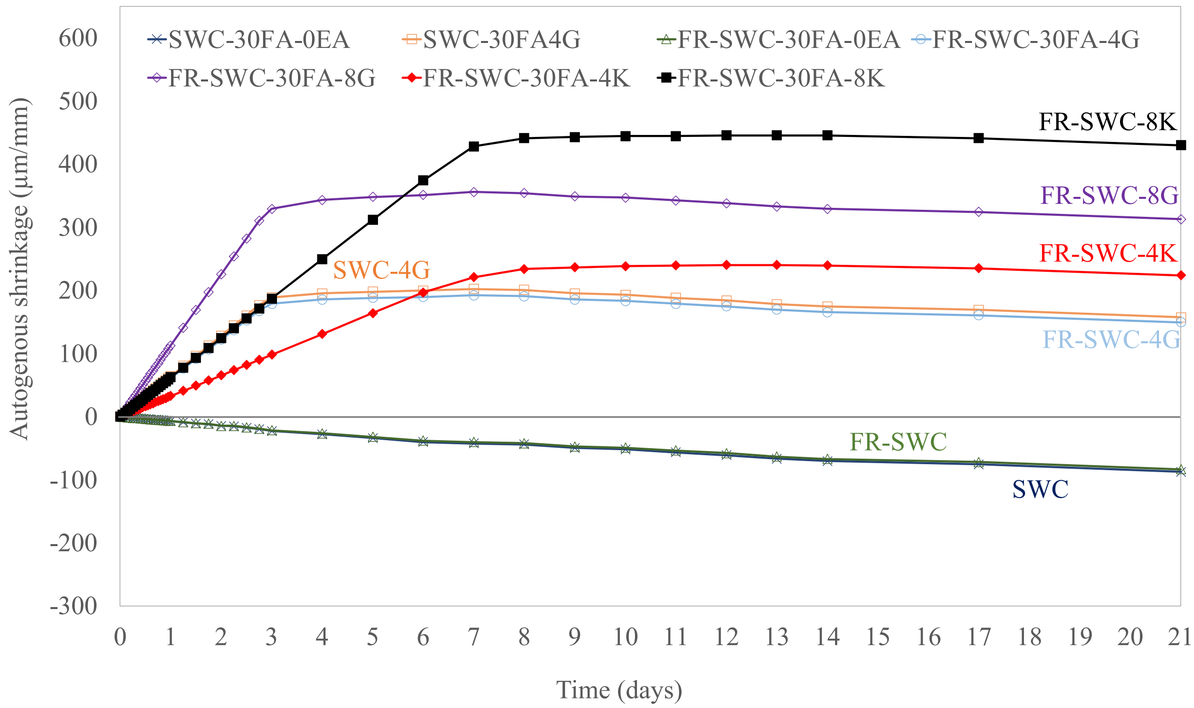


Autogenous shrinkage and expansion for selected FR-SWC mixtures up to 21 days (3-a)

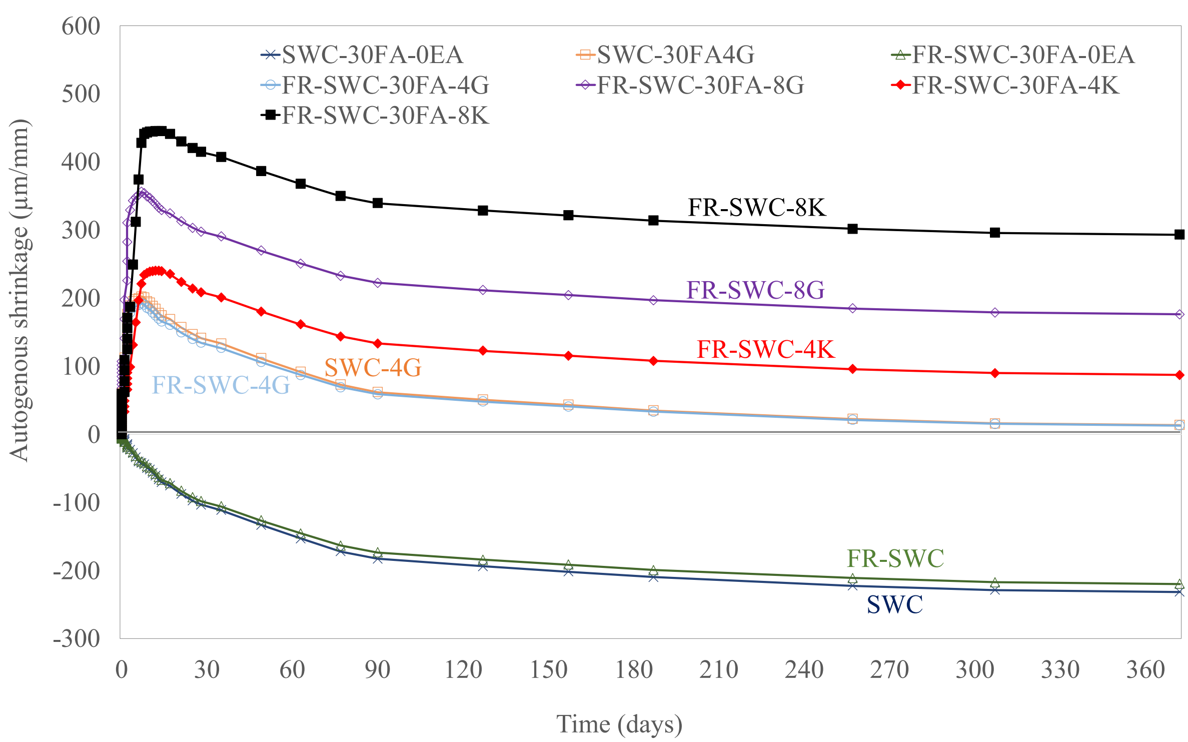


Autogenous shrinkage and expansion for selected FR-SWC mixtures up to 365 days (3-b)

**Fig. 3.** Autogenous shrinkage and expansion for selected FR-SWC mixtures. Autogenous shrinkage and expansion for selected FR-SWC mixtures up to 21 days (3-a), Autogenous shrinkage and expansion for selected FR-SWC mixtures up to 365 days (3-b).

50% FA replacement due to their higher mechanical properties and lower total binder content. The selected mixtures were tested for total shrinkage and autogenous shrinkage. Figs. 2 and 3 show the autogenous shrinkage over time for the FR-SCC and FR-SWC mixtures, respectively. The FR-SCC mixtures were shown to have higher expansion and higher shrinkage compared to similar FR-SWC mixtures and that can be due to the higher paste content in the FR-SCC mixtures compared to the FR-SWC mixtures. The 1-year autogenous shrinkage for the SCC and the FR-SCC mixtures made with no EA was about 250 micro-strains. On the other hand, these mixtures when prepared with EAs experienced a 1-year autogenous expansion that ranged from 150 to 375 micro-strains. In the case of the SWC and the FR-SWC, the mixtures prepared with EAs experienced a 1-year autogenous expansion that ranged from 20 to 475 micro-strains.

The FR-SCC and FR-SWC mixtures made with Type-K EA showed higher expansion compared to those made with Type-G EA. For mixtures

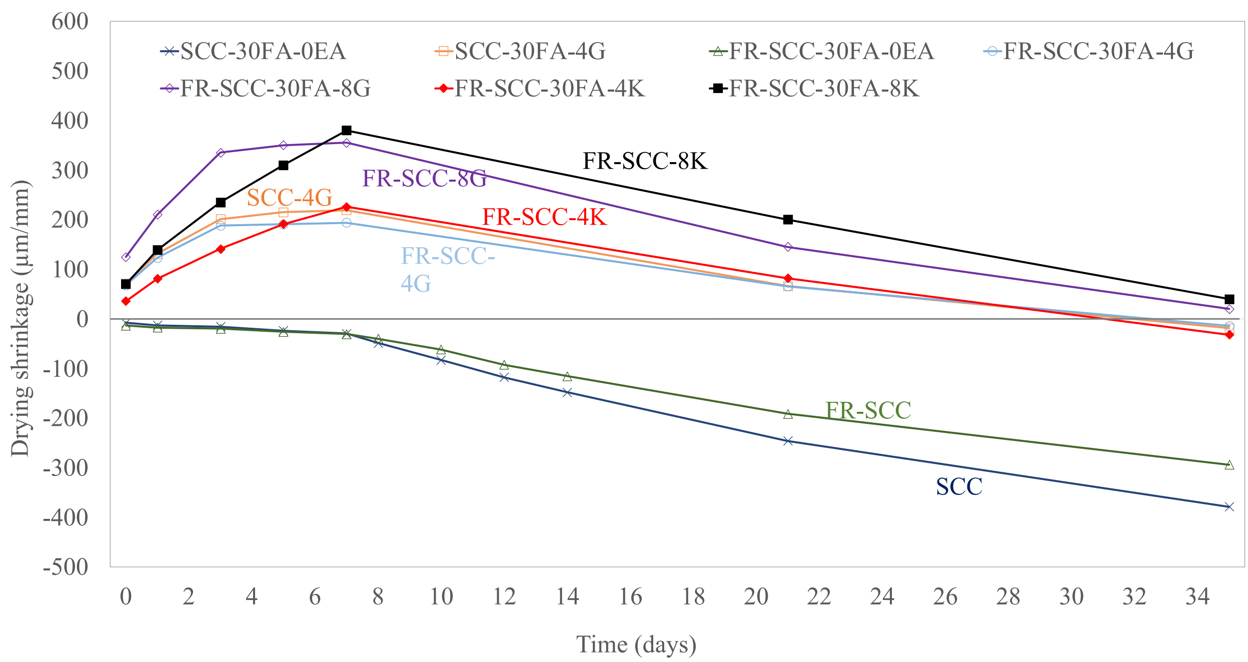


Total shrinkage and expansion for selected FR-SCC mixtures up to 35 days (4-a)

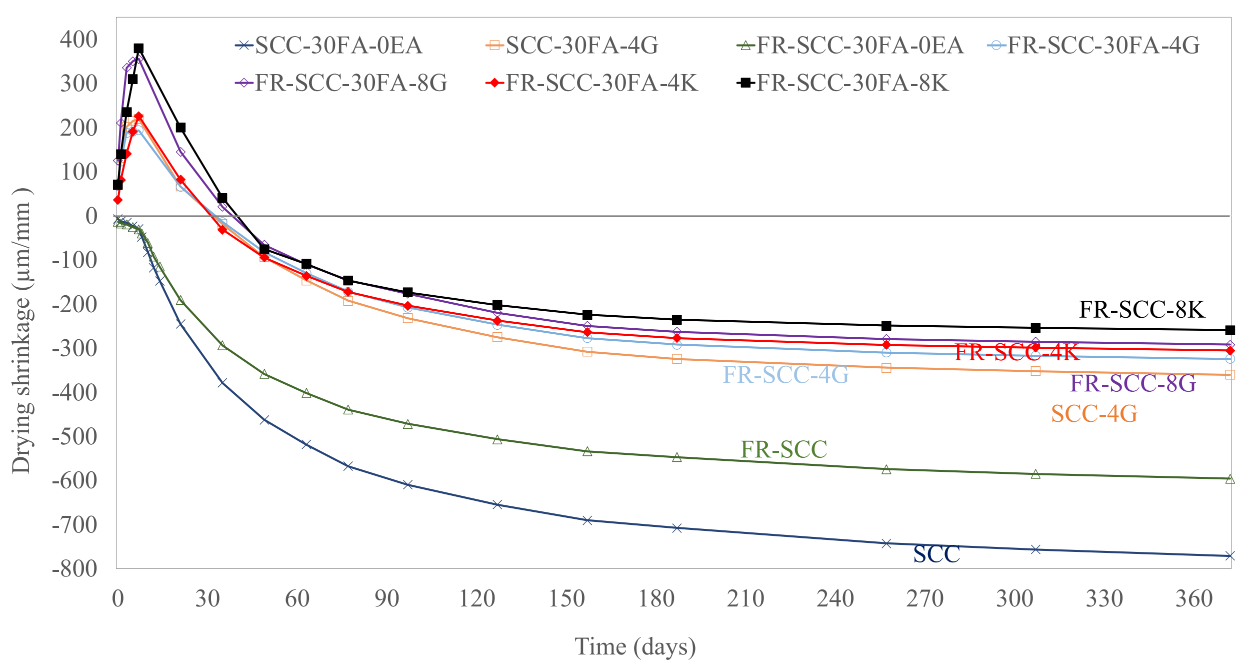


Total shrinkage and expansion for selected FR-SCC mixtures up to 365 days (4-b)

**Fig. 4.** Total shrinkage and expansion for selected FR-SCC mixtures. Total shrinkage and expansion for selected FR-SCC mixtures up to 35 days (4-a), Total shrinkage and expansion for selected FR-SCC mixtures up to 365 days (4-b).

made with Type-K EA, the expansion reached 500 and 440 micro-strains for FR-SCC and FR-SWC, respectively. Similar to the findings from previous studies [3], mixtures made with Type-G EA developed 95% of the expansion in the first three days, however the expansion rate beyond that third day of moist curing was not significant. Unlike the case with the mixtures made with Type-K EA in which the rate of expansion was constant over the seven days of moist curing.

The prismatic shrinkage samples were demolded after one day and the initial readings were recorded at that time. Since the investigated mixtures were prepared with EA and considerable strain was expected during the first day, the strain due to drying shrinkage of the prismatic shrinkage samples during the first day before demolding was neglected

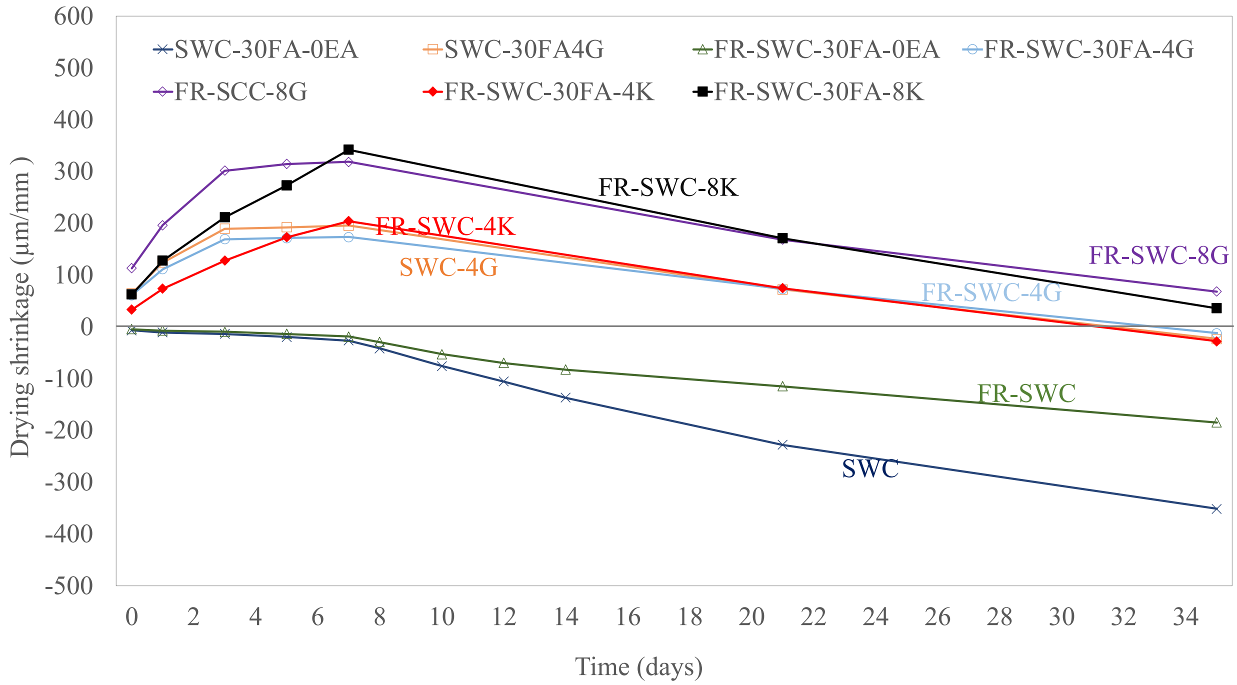


Total shrinkage and expansion for selected FR-SWC mixtures up to 35 days (5-a)

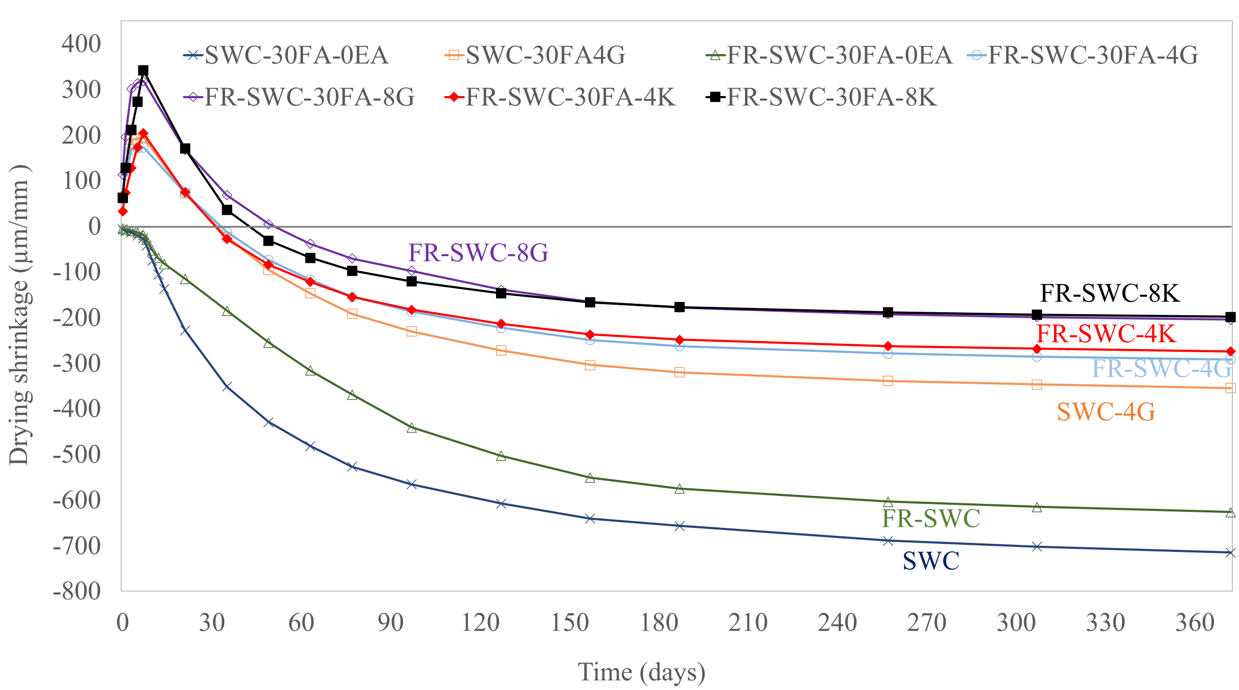


Total shrinkage and expansion for selected FR-SWC mixtures up to 365 days (5-b)

**Fig. 5.** Total shrinkage and expansion for selected FR-SWC mixtures. Total shrinkage and expansion for selected FR-SWC mixtures up to 35 days (5-a), Total shrinkage and expansion for selected FR-SWC mixtures up to 365 days (5-b).

compared to the autogenous shrinkage. Since no shrinkage reading was taken during the first day as the prismatic samples were still in molds, the strain of those prismatic samples during the first day was assumed to be equivalent to autogenous shrinkage of the tubular samples as the prisms were under curing during the first day and up to seven days. The total shrinkage at each day was determined as the summation of the first day autogenous shrinkage for the tubular samples and the shrinkage reading of the prismatic samples that started after the first day as shown in Figs. 4 and 5.

The presence of coarse aggregates and/or fibers are factor affecting expansion of concrete but they are not the major factors. The major factors that control expansion of concrete is the type of EA, content of EA, w/cm, and duration of moist curing. Therefore, the similarity between the autogenous deformation and drying deformation at the first 7 days is due to the fact that drying shrinkage samples were moist cured for 7 days without any drying which resulted in expansion close to the values of the same mixture in autogenous shrinkage test, that's why the highest autogenous deformation of sieved FR-SCC-30FA-8G and FR-SWC-30FA-8G sieved concrete mixtures were about 390 and 355 micro-strain as shown in Fig. 2 and Fig. 3. These data were close to the highest drying deformation of FR-SCC-30FA-8G and FR-SWC-30FA-8G concrete mixtures that were about 370 and 320 micro-strain as demonstrated by Fig. 4 and Fig. 5. The 1-year total shrinkage for the SCC and the FR-SCC mixtures made with no EA was 780 and 600 micro-strains, respectively. These mixtures when prepared with EAs experienced a 1-year total shrinkage that ranged from 250 to 375 micro-strains. In the case of the SWC and the FR-SWC, the mixtures prepared with EAs experienced a 1-year total shrinkage that ranged from 200 to 350 micro-strains. FR-SCC and FR-SWC Mixtures made with fibers and EA exhibited up to 60% lower total shrinkage after one year compared to similar non-fibrous mixtures made with no EA. The type and the dosage of the EA had no significant effect on such reduction. Fig. 4-b and 5-b show the first 35 days of shrinkage deformation for the FR-SCC and FR-SWC mixtures. The use of fibers decreased the expansion for mixtures made with EA and fibers, but it had a positive impact on shrinkage reduction. The net effect of using fibers and EA had the most significant effect on decreasing the total shrinkage (up to 60% depending on the type of EA and the type of concrete). The incorporation of fibers without EA decreased the total shrinkage by 20% in the case of FR-SCC and by 10% in the case of FR-SWC. The use of 4% Type-G EA without fibers decreased the total shrinkage by about 50% for both concrete types. As in the case of autogenous shrinkage, mixtures made with Type-G EA developed around 95% of the expansion in the first three days, in agreement with previous studies [3], and the mixtures made with Type-K EA had a constant rate of expansion over the seven days of moist curing.

All mixtures made with either type of EA showed sharp drop in total shrinkage. However, mixtures made with Type-G EA were further developed given the sharp loss in workability associated with the use of Type-K EA. The FR-SCC and FR-SWC mixtures made with 4% Type-G EA were selected over those with 8% Type-G EA since the lower EA dosage resulted in slightly greater mechanical properties and adequate shrinkage performance.

### 4.4. Elastic modulus

Based on the workability and mechanical performance, four optimized FR-SCC mixtures were selected to evaluate the elastic modulus and restrained shrinkage characteristics, as shown in Table 5. The elastic modulus was tested after 3, 7, 28, 56, and 91 days of moist curing.

Table 5 shows the variations in elastic modulus with time results for the investigated mixtures. The 3-day elastic modulus varied between 15.5 and 18.2 GPa with the FR-SCC mixture made with EA recording the highest value of 18.2 GPa. The 91-day elastic modulus varied between 28.2 and 30.9 GPa with the SCC mixture made with EA recording the highest value of 30.9 GPa. Neither fiber nor EA had a significant effect on the elastic modulus at any age for the five investigated concrete mixtures; the variation of the elastic modulus between the mixtures was ± 2.7 GPa.

### 4.5. Restrained shrinkage

The steel ring strain profiles of the five selected mixtures in the restrained shrinkage test are plotted in Fig. 6. The cracking potential of concrete dependents on several factors that includes autogenous and drying shrinkage, modulus of elasticity, tensile strength, and creep. As expected, the SCC mixture without any EA and fiber exhibited the lowest restrained shrinkage resistance and had a $t_{cr}$ of 12.5 days given its highest shrinkage and elastic modulus at early age, and lowest tensile strength. The SWC mixture, with a lower cement content compared to SCC, exhibited lower shrinkage and higher restrained shrinkage resistance with $t_{cr}$ of 16.5 days compared to SCC mixture with $t_{cr} = 12.5$ day. The use of EA without fibers increased the $t_{cr}$ to be 20 days; that increase was lower in the case of using fibers but no EA ($t_{cr} = 17$ day). These results are in agreement with Soo-Duck and Khayat (2014) [38,39]. The combined use of fibers and EA led to the highest enhancement of restrained shrinkage resistance with $t_{cr} = 36.5$ day. This is due to the prestressing effect of the fibers, which is associated with the initial expansion of the cement paste. This can increase the tensile strength of the FRC and its resistance to cracking. As a result, the fibers in the FR-SCC-30FA-4G mixture can fail at higher stress corresponding to fiber pre-stressing plus fiber strength compared to similar concrete with an EA, as is the case of the FR-SCC-30FA-0EA mixture.

Fig. 7 shows a direct relationship between time to crack and crack width. The maximum first crack width of 170 $\mu m$ was measured at $t_{cr} = 12.5$ day for the SCC mixture without any fibers and EA. The narrowest first crack width of 85 $\mu m$ was measured at $t_{cr} = 36.5$ day for the FR-SCC mixture made with EA and fibers. All non-fibrous mixtures exhibited enlargement of the first crack that reached a value between 480 and 520 mm at 50 days. On the other hand, the first crack width of the fibrous mixtures remained constant up to 50 days. This is because of the crack obstruction due to the presence of the fibers in the FR-SCC and FR-SWC mixtures. Once concrete reached tensile strength and first crack-initiated, steel fibers started to bridge that crack and carried the load, hence prevented further enlargement or propagation of the crack. The use of micro fibers in combination with macro fibers and increasing the curing period up to seven days instead of three days will prevent concrete from cracking [40].

The induced tensile stress due to the restrained shrinkage of concrete

**Table 5**
Elastic modulus and restrained shrinkage results

| Mixture abbreviation | E 3 d (GPa) | E 7 d (GPa) | E 28 d (GPa) | E 56 d (GPa) | E 91 d (GPa) | $t_{cr}$ (day) | First crack Width (μm) | Max. crack Width at 50-days (μm) |
|---|---|---|---|---|---|---|---|---|
| SCC-30FA-0EA | 17.5 | 22.1 | 26.7 | 29.3 | 29.9 | 12.5 | 170 | 520 |
| SCC-30FA-4G | 18.1 | 22.9 | 27.2 | 30.3 | 30.9 | 20.0 | 125 | 490 |
| FR-SCC-30FA-0EA | 17.7 | 22.2 | 26.6 | 28.1 | 28.6 | 17.0 | 135 | 135 |
| FR-SCC-30FA-4G | 18.2 | 22.4 | 26.3 | 27.8 | 28.2 | 36.5 | 80 | 80 |
| SWC-30FA-0EA | 15.5 | 20.2 | 25.9 | 27.9 | 28.6 | 16.5 | 140 | 480 |

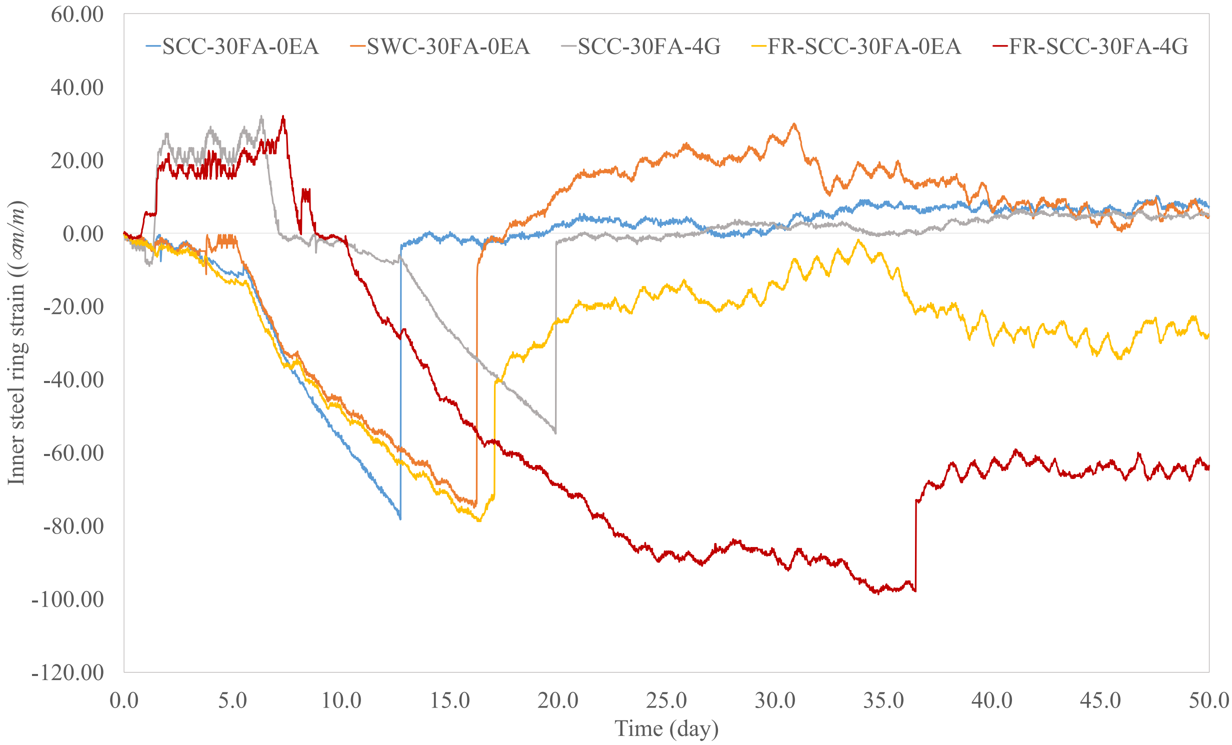


**Fig. 6.** Variations of steel ring strain due to shrinkage of concrete ring as a function of time.

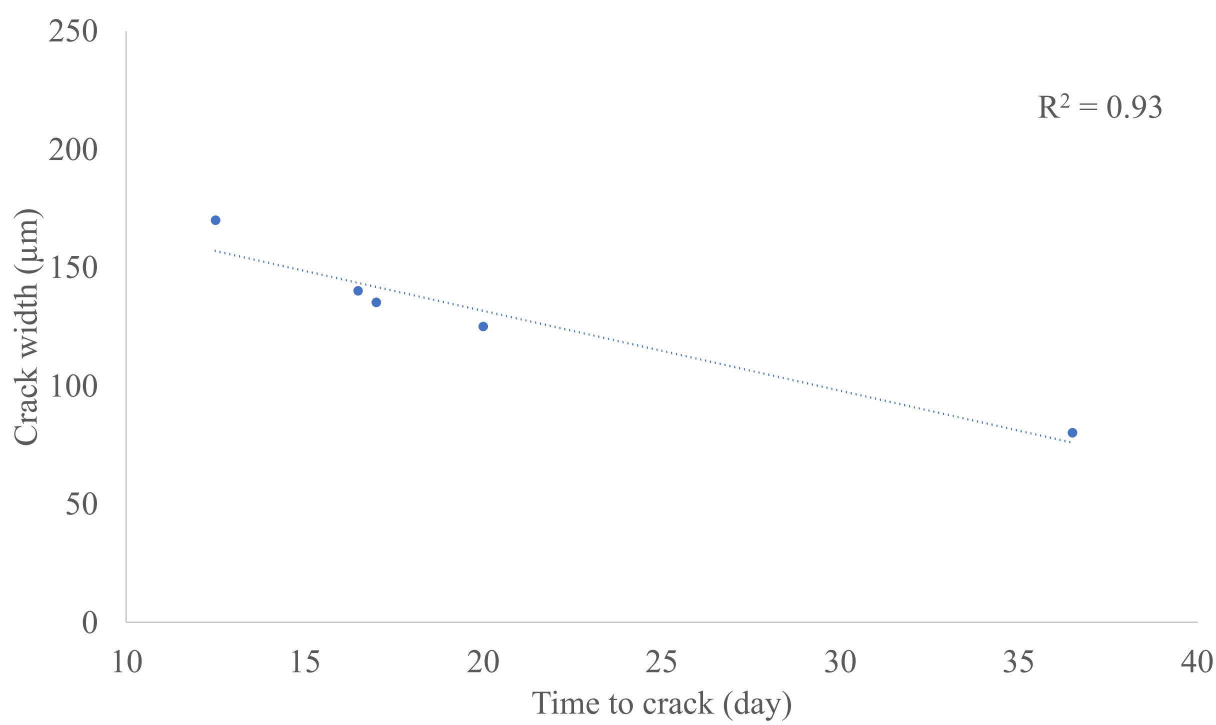


**Fig. 7.** Time to crack vs. first crack width.

can be calculated by knowing the measurements of the concrete and the steel rings as well as the elastic modulus of the steel ring using Equations (11) and (12) [41,42].

$$\sigma_t(t) = G\varepsilon_{st}(t) = G\left[\varepsilon_{sh}(t) - \varepsilon_e(t) - \varepsilon_{cp}(t)\right] \quad (11)$$

$$G = \frac{E_{st} r_{ic} h_{st}}{r_{is} h_c} \quad (12)$$

where $\varepsilon_{st}$ *(t)* is the steel ring strain at time *t*; $\varepsilon_{cp}$ *(t)*, $\varepsilon_{sh}$ *(t)*, and $\varepsilon_e$ *(t)* are tensile creep strain, the free total deformation strain, and elastic strain,

respectively, at time $t$; $E_{st}$ = elastic modulus of the steel ring (200 GPa); $G$ is a constant for the ring properties and dimensions; and $h_c$ and $h_{st}$ are the thicknesses of the concrete and steel rings, respectively; $r_{ic}$ and $r_{is}$ refer to the inner radii of the concrete and steel, respectively.

Fig. 8 shows the induced tensile stress in the concrete that was computed using the steel ring strain shown in Fig. 5. Unlike non-fibrous SCC, the FR-SCC mixture made with EA was able to resist more induced tensile stresses due to shrinkage after cracking, while the non-fibrous SCC and SWC mixtures did not resist any tensile stress beyond cracking.

Fig. 9 shows the shrinkage cracking resistance index, which consists of the integration of induced tensile stress over time during restrained shrinkage testing. The FR-SCC mixture made with the optimized EA showed the highest index. In the case of fibrous mixtures, the index increased with time since these mixtures were able to restrain loads after cracking. On the other hand, the index did not increase with time in the case of the non-fibrous mixtures. Once the non-fibrous SCC and SWC rings cracked, the shrinkage cracking resistance index started to be constant.

### 4.6. Tensile creep coefficient

Knowing the variations in strain of the steel ring (Fig. 5), total deformation of concrete (Fig. 4), and elastic modulus of concrete (Table 5), the variations of tensile creep coefficient ($C_r(t)$) of the investigated mixtures can be calculated using Equation (13) [5,43], where $E_c(t)$ is the modulus of elasticity of the concrete at time $t$.

$$C_r(t) = \frac{E_c(t) r_{is} h_c}{E_{st} r_{ic} h_{st}} \left[ \frac{\varepsilon_{sh}(t)}{\varepsilon_{st}(t)} - 1 \right] - 1 \quad (13)$$

Fig. 10 shows the variations of the calculated $C_r(t)$ for the investigated mixtures. The $C_r(t)$ is one of the factors affecting the risk of cracking under restrained shrinkage, in addition to total shrinkage, tensile strength, and elastic modulus [44]. Similarly, concrete mixtures with higher total shrinkage and elastic modulus can exhibit higher cracking potential if the other two factors (tensile strength and $C_r(t)$) are constant. Concrete with higher tensile strength and $C_r(t)$ can develop lower cracking potential if the other two factors (total shrinkage and elastic modulus) are constant.

The values of the stabilized tensile creep coefficient ($C_r$) for the tested mixtures varied between 0.30 and 0.45. The lower total binder content in the non-fibrous SWC mixture compared to the SCC mixture led to lower $C_r$. The lower total shrinkage of the SWC compared to SCC resulted in lower cracking potential with $t_{cr}$ of 16.5 vs. 12.5 days, respectively. The incorporation of EA slightly increased $C_r$ and led to a 50% reduction in total shrinkage; the net effect on restrained shrinkage was positive with an increase in $t_{cr}$ from 12.5 to 20 days. The use of fibers significantly increased the splitting tensile strength of the FR-SCC-30FA-0EA mixture by 40% and $C_r$ by 12.5% compared to the reference SCC-30FA-0EA mixture; the net effect was an increase of $t_{cr}$ from 12.5 to 17 days. Combining the use of EA with fibers in the FR-SCC-30FA-4G mixture provided the concrete with 45% higher tensile strength, 7.5% higher $C_r$, and 60% lower total shrinkage, which resulted in lower cracking potential with an increase in $t_{cr}$ from 12.5 to 36.5 days.

## 5. Conclusions

A comprehensive study was carried out for optimized FR-SCC and FR-SWC mixtures to investigate the effect of fiber and/or EA type and dosage on key factors affecting key fresh and hardened concrete properties. Based on the test results reported herein, the following conclusions can be warranted:

1. The 24 investigated FR-SCC and FR-SWC mixtures had acceptable passing ability values ($D/a$) varying between 12.1 and 14.7. The binder composition did not have a significant effect on passing ability.
2. The use of Type-K EA led to high degree of workability loss compared to the reference mixture made without any EA or with Type-G EA. The FR-SCC mixture made without any EA had 22% lower slump flow after 60 min. Such loss was 8% in the case of the FR-SCC mixture made with 4% Type-G EA compared to 50% in the case of 8% Type-K EA.

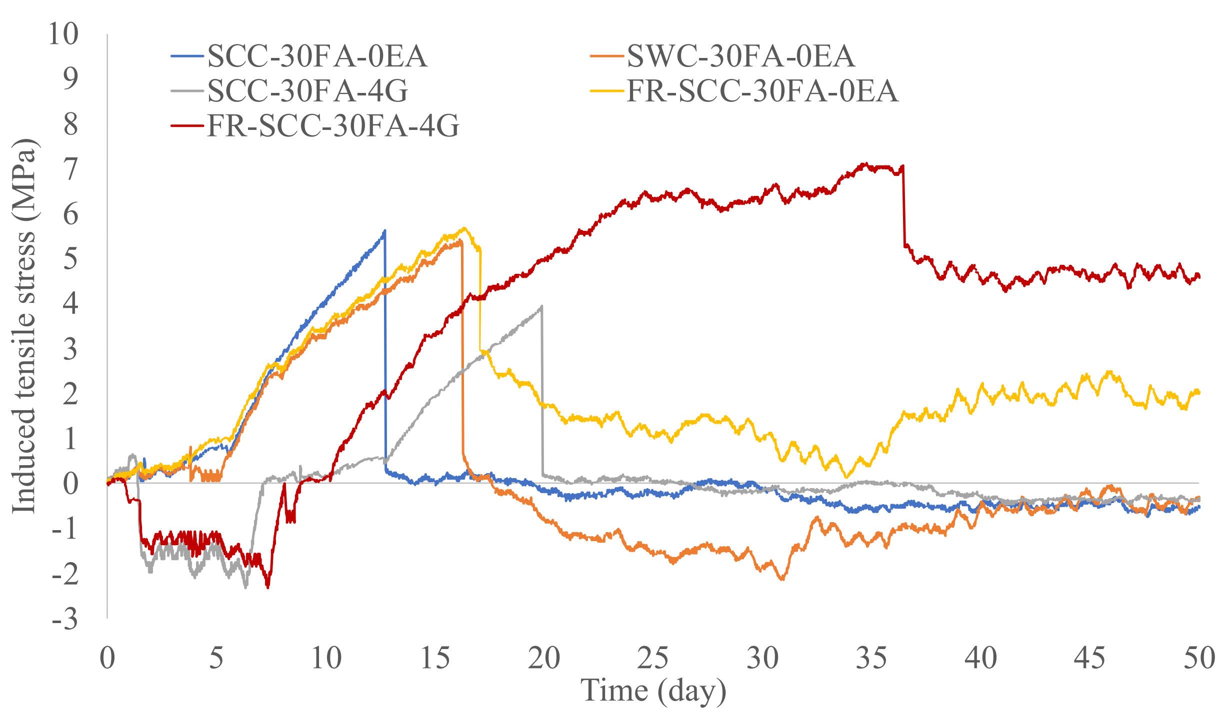


**Fig. 8.** Induced tensile stress due to shrinkage of concrete as a function of time.

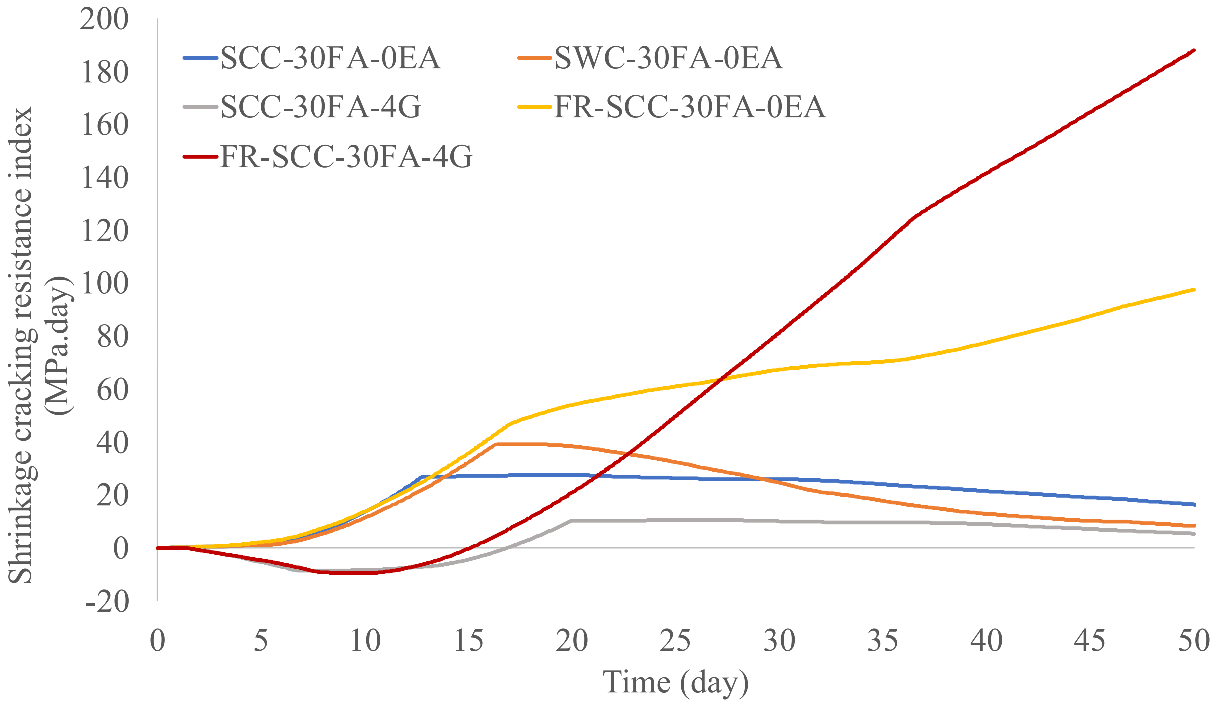


**Fig. 9.** Shrinkage cracking resistance index as a function of time.

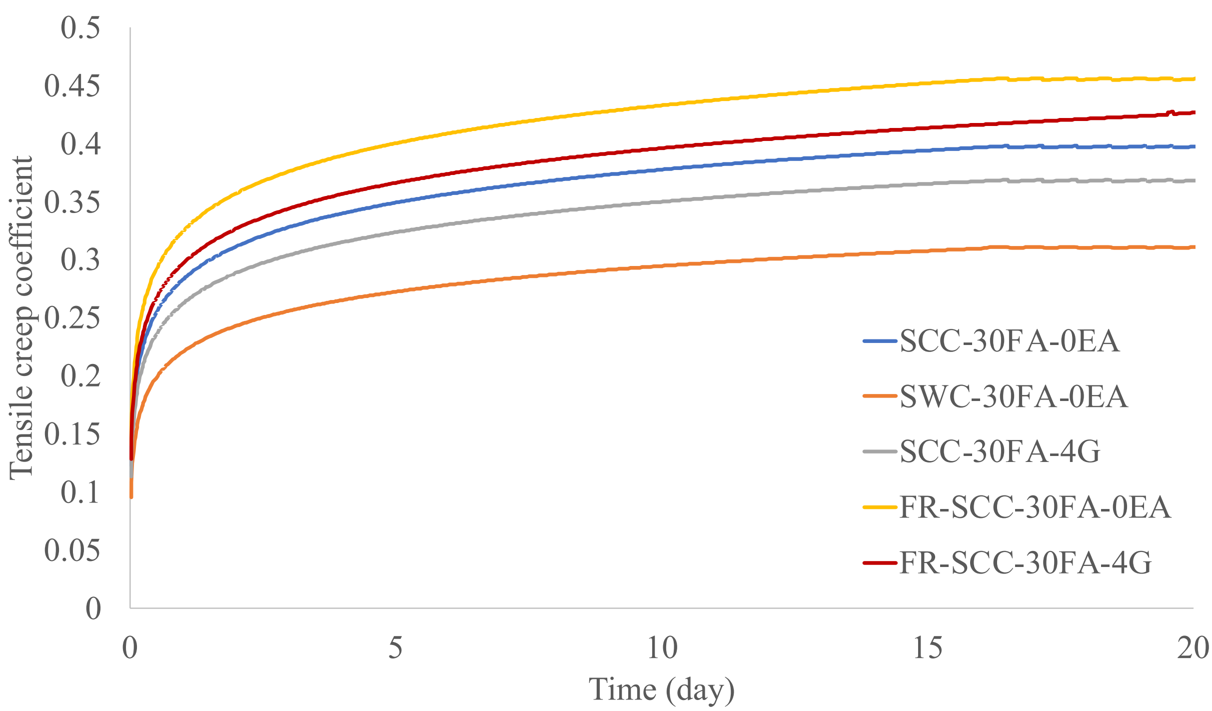


**Fig. 10.** Variations of tensile creep coefficient as a function of time.

3. The optimized binder content for the FR-SWC mixture was 380 kg/$m^3$ that contained 30% Class C FA and 4% Type-G EA, by mass. The binder composition of the optimized FR-SCC was the same as the FR-SWC; however, the total binder content was 475 kg/$m^3$.
4. The synergetic effect of fiber and EA had a significant effect on mechanical properties with 40% increase in splitting tensile strength of the FR-SCC and 60% in the case of FR-SWC.
5. Mixtures made with Type-G EA developed 95% of the expansion in the first 3 days of moist curing, whereas those prepared with Type-K EA had constant rate of expansion over 7 days of moist curing.
6. The use of fibers in the absence of EA decreased the total shrinkage by 20% in the case of FR-SCC and by 10% for FR-SWC. The addition of 4% Type-G EA without any fibers decreased the total shrinkage by about 50% for both concrete types. The coupled effect of EA and

fibers decreased the total shrinkage by up to 60% compared to reference SWC or SCC mixtures.

7. The incorporation of EA decreased the $C_r$ of SCC by 10% and significantly decreased the total shrinkage by 50% resulting in increasing $t_{cr}$ from 12.5 to 20 days.
8. The use of fibers increased the splitting tensile strength of SCC by 40% and $C_r$ by 13% leading to increase in $t_{cr}$ from 12.5 to 36.5 days.
9. Combining the EA with fibers provided FR significant enhancement in performance (45% higher tensile strength, 8% higher $C_r$, and 60% lower total shrinkage) leading to the lowest cracking potential and highest $t_{cr}$ of 36.5 days.

*CRediT authorship contribution statement*

**Ahmed Abdelrazik:** Data curation, Software, Validation, Visualization, Investigation, Writing – review & editing. **Kamal H. Khayat:** Conceptualization, Methodology, Supervision.

## Declaration of Competing Interest

The authors declare that they have no known competing financial interests or personal relationships that could have appeared to influence the work reported in this paper.

## Acknowledgements

The authors would like to greatly acknowledge the support of the Research on Concrete Applications for Sustainable Transportation (RE-CAST) Tier-1 University Transportation Center (UTC), Missouri Department of Transportation (MoDOT) (Grant# TR2015-05), and the Center for Infrastructure Engineering Studies (CIES) at Missouri University of Science and Technology.

## References

[1] Mikanovic N, Leclerc A, Ponge A, Khayat K. Workability characteristics and performance criteria for design and control of superworkable concrete, InSixth International RILEM Symposium on Self-Compacting Concrete and 4th North American Conference on the Design and Use of SCC, Montreal, Canada 2010.
[2] K.H. Khayat, F. Kassimi, P. Ghoddousi, Mixture design and testing of fiber-reinforced self-consolidating concrete, ACI Mater. J. 111 (2) (2014 Mar 1) 143.
[3] P. Gao, X. Lu, F. Geng, X. Li, J. Hou, H. Lin, N. Shi, Production of MgO-type expansive agent in dam concrete by use of industrial by-products, Build. Environ. 43 (4) (2008) 453–457.
[4] W. Sun, H. Chen, X. Luo, H. Qian, The effect of hybrid fibers and expansive agent on the shrinkage and permeability of high-performance concrete, Cem. Concr. Res. 31 (4) (2001) 595–601.
[5] Kassimi F, Khayat KH. Effect of Fiber and Admixture Types on Restrained Shrinkage Cracking of Self Consolidating Concrete. InFifth North American Conference on the Design and Use of Self-Consolidating Concrete, Chicago, Illinois, USA 2013.
[6] H.T. See, E.K. Attiogbe, M.A. Miltenberger, Potential for restrained shrinkage cracking of concrete and mortar, Cement, concrete and aggregates. 26 (2) (2004) 1–8.
[7] Z. Pan, Y. Zhu, D. Zhang, N. Chen, Y. Yang, X. Cai, Effect of expansive agents on the workability, crack resistance and durability of shrinkage-compensating concrete with low contents of fibers, Constr. Build. Mater. 259 (2020) 119768, https://doi.org/10.1016/j.conbuildmat.2020.119768.
[8] Q. Cao, Q. Gao, J. Jia, R. Gao, Early-Age Cracking Resistance of Fiber-Reinforced Expansive Self-Consolidating Concrete, ACI Mater. J. 116 (1) (2019) 15–26.
[9] C. Li, P. Shang, F. Li, M. Feng, S. Zhao, Shrinkage and mechanical properties of self-compacting SFRC with calcium-sulfoaluminate expansive agent, Materials. 13 (3) (2020 Jan) 588.
[10] Q.i. Cao, Q. Gao, R. Wang, Z. Lin, Effect of fibers and expansive agent on shrinkage of self-consolidating concrete under two curing schemes, J. Mater. Civ. Eng. 31 (9) (2019) 04019204, https://doi.org/10.1061/(ASCE)MT.1943-5533.0002761.
[11] V. Corinaldesi, A. Nardinocchi, Mechanical characterization of Engineered Cement-based Composites prepared with hybrid fibres and expansive agent, Compos. B Eng. 1 (98) (2016 Aug) 389–396.
[12] J.-J. Park, D.-Y. Yoo, S.-W. Kim, Y.-S. Yoon, Drying shrinkage cracking characteristics of ultra-high-performance fibre reinforced concrete with expansive and shrinkage reducing agents, Mag. Concr. Res. 65 (4) (2013) 248–256.
[13] R.Z. Dong, J. Wei, Y.X. Qi, L.T. Guo, B. Chen, Y. Liu, R. Wei, Compensation effect of expansive agent on shrinkage of self-compacting concrete. InApplied Mechanics and Materials, Trans Tech Publications Ltd. 507 (2014) 401–405.
[14] P. Gao, X. Lu, M. Tang, Shrinkage and expansive strain of concrete with fly ash and expansive agent, Journal of Wuhan University of Technology-Mater. Sci. Ed. 24 (1) (2009) 150–153.
[15] G. Zhang, G. Li, Effects of mineral admixtures and additional gypsum on the expansion performance of sulphoaluminate expansive agent at simulation of mass concrete environment, Constr. Build. Mater. 15 (113) (2016 Jun) 970–978.
[16] A. Wang, M. Deng, D. Sun, L. Mo, J. Wang, M. Tang, Effect of combination of steel fiber and MgO-type expansive agent on properties of concrete, Journal of Wuhan University of Technology-Mater. Sci. Ed. 26 (4) (2011) 786–790.
[17] A.T. Abdelrazik, K.H. Khayat, Effect of fiber characteristics on fresh properties of fiber-reinforced concrete with adapted rheology, Constr. Build. Mater. 230 (2020) 116852, https://doi.org/10.1016/j.conbuildmat.2019.116852.
[18] K. Khayat, F. Kassimi, O. Bonneau, Consolidation of test samples made with fiber-reinforced superworkable concrete, In12th International Conference for Recent Advances in Concrete Technology and Sustainability Issues, Czech Republic, Prague, 2012.
[19] K.H. Khayat, N. Petrov, A.J. Morin, M. Thibault, Performance of SCC used in the repair of retaining wall elements, SCC 2005 (2005) 1003–1013.
[20] K.H. Khayat, A. Abdelrazik, Field Implementation of Super-Workable Fiber-Reinforced Concrete for Infrastructure Construction. Missouri University of Science and Technology, Dept. of Civil, Architectural, and Environmental Engineering (2019). Jan 1.
[21] ASTM, C1611/ C1611M–09b, Standard test method for slump flow of self-consolidating concrete, ASTM International, PA (2009) 6.
[22] F. Kassimi, K.H. Khayat, Development of methodology to evaluate passing ability and test sample preparation for superworkable concrete, Constr. Build. Mater. 20 (183) (2018 Sep) 356–364.
[23] ASTM C1621/C1621M-09b, Standard test method for passing ability of self-consolidating concrete by J-Ring, ASTM International, PA, 2014, p. 5.
[24] ASTM C232/C232M-14, Standard test method for bleeding of concrete, ASTM International, PA, 2014, p. 3.
[25] EPG (Self-Compacting Concrete European Project Group), The European Guidelines for Self-Compacting Concrete, Experts for Specialized Construction and Concrete Systems (EFNARC), Farnham, UK 2005.
[26] ASTM C138/C138M-13a, Standard test method for density (unit weight), yield, and air content (gravimetric) of concrete, ASTM International, PA, 2014, p. 4.
[27] ASTM C231/C231M-10, Standard test method for air content of freshly mixed concrete by the pressure method, ASTM International, PA, 2009, p. 10.
[28] ASTM C39/C39M-14, Standard test method for compressive strength of cylindrical concrete specimens, ASTM International, PA, 2014, p. 7.
[29] ASTM C496/C496M-11, Standard test method for splitting tensile strength of cylindrical concrete specimens, ASTM International, PA, 2011, p. 5.
[30] ASTM C469/C469M-14, Standard test method for static modulus of elasticity and Poisson's ratio of concrete in compression, ASTM International, PA, 2014, p. 5.
[31] ASTM C157/C157M-08, Standard test method for length change of hardened hydraulic-cement mortar and concrete, ASTM International, PA, 2008, p. 7.
[32] ASTM C1698/C1698M-09, Standard test method for autogenous strain of cement paste and mortar, ASTM International, PA, 2014, p. 8.
[33] ASTM C1581/C1581M-09a, Standard test method for determining age at cracking and induced tensile stress characteristics of mortar and concrete under restrained shrinkage, ASTM International, PA, 2014, p. 7.
[34] T. Voigt, V.K. Bui, S.P. Shah, Drying shrinkage of concrete reinforced with fibers and welded-wire fabric, Materials Journal. 101 (3) (2004 May 1) 233–241.
[35] ASTM C29/C29M-09, Standard test method for bulk density (unit weight) and voids in aggregate, ASTM International, PA, 2012, p. 5.
[36] S. Nagataki, H. Gomi, Expansive admixtures (mainly ettringite), Cem. Concr. Compos. 20 (2-3) (1998) 163–170.
[37] C. Jakob, D. Jansen, N. Ukrainczyk, E. Koenders, U. Pott, D. Stephan, J. Neubauer, Relating ettringite formation and rheological changes during the initial cement hydration: a comparative study applying XRD analysis, rheological measurements and modeling, Materials. 12 (18) (2019 Jan) 2957.
[38] S.-D. Hwang, K.H. Khayat, Effect of mix design on restrained shrinkage of self-consolidating concrete, Mater. Struct. 43 (3) (2010) 367–380.
[39] S.D. Hwang, K.H. Khayat, Effect of mixture composition on restrained shrinkage cracking of self-consolidating concrete used in repair, ACI Mater. J. 105 (5) (2008 Sep 1) 499.
[40] Khayat KH, Abdelrazik A. Performance of Fiber-Reinforced Self-Consolidating Concrete for Repair of Bridge Sub-Structures and Fiber-Reinforced Super-Workable Concrete for Infrastructure Construction. 2017 Sep.
[41] Ulm FJ, Bažant ZP, Wittmann FH, Bazant ZP. Creep, shrinkage and durability mechanics of concrete and other quasi-brittle materials.
[42] W.J. Weiss, S. Ferguson, Restrained shrinkage testing: the impact of specimen geometry on quality control testing for material performance assessment, Concreep. 6 (2001 Aug) 645–651.
[43] H.T. See, E.K. Attiogbe, M.A. Miltenberger, Shrinkage cracking characteristics of concrete using ring specimens, Materials Journal. 100 (3) (2003 May 1) 239–245.
[44] I. Mehdipour, K.H. Khayat, Elucidating the role of supplementary cementitious materials on shrinkage and restrained-shrinkage cracking of flowable eco-concrete, J. Mater. Civ. Eng. 30 (3) (2018) 04017308, https://doi.org/10.1061/(ASCE)MT.1943-5533.0002191.